

## **General Disclaimer**

### **One or more of the Following Statements may affect this Document**

- This document has been reproduced from the best copy furnished by the organizational source. It is being released in the interest of making available as much information as possible.
- This document may contain data, which exceeds the sheet parameters. It was furnished in this condition by the organizational source and is the best copy available.
- This document may contain tone-on-tone or color graphs, charts and/or pictures, which have been reproduced in black and white.
- This document is paginated as submitted by the original source.
- Portions of this document are not fully legible due to the historical nature of some of the material. However, it is the best reproduction available from the original submission.

"Made available under NASA sponsorship  
in the interest of early dissemination of  
information of Earth Resources  
Program information and data  
for any use made thereof."

(E79-10257) EVALUATION OF LANDSAT  
MULTISPECTRAL SCANNER IMAGES FOR MAPPING  
ALTERED ROCKS IN THE EAST TINTIC MOUNTAINS,  
UTAH (Geological Survey, Reston, Va.) 136 p  
HC A07/MF A01

CSCL 08G G3/43

Unclas  
00257

~~SECRET~~  
7.0-10.257

N79-31717-63

EVALUATION OF LANDSAT MULTISPECTRAL SCANNER IMAGES  
FOR MAPPING ALTERED ROCKS IN  
THE EAST TINTIC MOUNTAINS, UTAH

by

Lawrence C. Rowan  
U. S. Geological Survey, Reston, Virginia

and

Michael J. Abrams  
Jet Propulsion Laboratory, Pasadena, California

**ORIGINAL CONTAINS  
COLOR ILLUSTRATIONS**

U. S. Geological Survey Open File Report 78-736

23890

Original photography may be purchased from:  
EROS Data Center

Sioux Falls, SD 57199

RECEIVED

JUN 06 1979

SIS/902.6

## Table of Contents

	<u>Page</u>
Abstract . . . . .	i
Introduction . . . . .	1
Acknowledgements . . . . .	4
Lithology. . . . .	5
Sedimentary rocks . . . . .	5
Igneous rocks . . . . .	9
Hydrothermally altered rocks. . . . .	18
<u>Vegetation . . . . .</u>	<u>27</u>
Spectral reflectance . . . . .	35
Image analysis . . . . .	40
Color photographs . . . . .	40
MSS images. . . . .	44
Individual MSS band images . . . . .	45
Color-ratio composite images . . . . .	50
Evaluation of limonitic bedrock map. . . . .	56
East Tintic mining district. . . . .	65
Conclusions. . . . .	68
References cited . . . . .	71

## List of Figures

	<u>Page</u>
Figure 1 - Index map of the Great Basin . . . . .	1A
Figure 2 - Index map of the central part of the East Tintic Mountains. . . . .	1B
Figure 3 - Generalized geologic map . . . . .	2A
Figure 4 - Map of silicified rocks, veins and dikes . . . . .	18A
Figure 5 - Alteration map of the East Tintic Mining District . . . . .	20A
Figure 6 - Representative <u>in situ</u> reflectance spectra for unaltered and weathered quartz latite. . . . .	31A
Figure 7 - Representative <u>in situ</u> reflectance spectra for quartz latite subjected to accelerated weathering . . . . .	32A
Figure 8 - Representative <u>in situ</u> reflectance spectra for calcitic quartz latite . . . . .	33A
Figure 9 - Representative <u>in situ</u> reflectance spectra for argillized latitic tuff. . . . .	33B
Figure 10 - Representative <u>in situ</u> reflectance spectra for argillized latitic tuff. . . . .	34A
Figure 11 - Representative <u>in situ</u> reflectance spectra for argillized quartz latitic tuff . . . . .	34B
Figure 12 - Representative <u>in situ</u> reflectance spectra for intensely argillized quartz latite tuffs and flows . . . . .	35A

	<u>Page</u>
Figure 13 - Representative <u>in situ</u> reflectance spectra for silicified rocks . . . . .	35B
Figure 14 - Representative <u>in situ</u> reflectance spectra for limestones . . . . .	36A
Figure 15 - Representative <u>in situ</u> reflectance spectra for dolomites. . . . .	37A
Figure 16 - Representative <u>in situ</u> reflectance spectra for sage and juniper . . . . .	38A
Figure 17 - Skylab S190-B color photograph. . . . .	41A
Figure 18 - High-altitude color photograph. . . . .	42A
Figure 19 - Linearly stretched MSS band 5 image . . . . .	46A
Figure 20 - Density sliced MSS band 5 image . . . . .	47A
Figure 21 - Color-infrared composite image. . . . .	49A
Figure 22 - Schematic frequency distributions for MSS ratios 4/5, 5/6, 6/7, and 4/6 . . . . .	52A
Figure 23 - Color-ratio composite image . . . . .	55A
Figure 24 - Map showing the distribution of green pixels. . . .	55B
Figure 25 - Map showing distribution of green pixels representing limonitic bedrock . . . . .	55C
Figure 26 - Map comparing altered rocks mapped in the field with pixels representing limonitic bedrock . . . . .	56A
Figure 27 - Limonitic bedrock map of the East Tintic mining district . . . . .	66A
Figure 28 - Low-altitude color photograph of the East Tintic mining district. . . . .	67A

## List of Tables

	<u>Page</u>
Table 1 - Brief descriptions of geologic units . . . . .	5A
Table 2 - Paragenesis of alteration and ore minerals . . . . .	21A
Table 3 - Parameters for linear stretches used for black-and- white MSS images of the study area. . . . .	54A

Evaluation of Landsat Multispectral Scanner Images  
For Mapping Altered Rocks  
in the East Tintic Mountains, Utah

by

Lawrence C. Rowan, U.S. Geological Survey, Reston, VA  
Michael J. Abrams, Jet Propulsion Laboratory, Pasadena, CA

ABSTRACT

The East Tintic Mountains, Utah consist of folded and faulted Paleozoic sedimentary rocks, which are partly covered by Tertiary volcanic rocks. Clastic rocks dominate the lower one-third of the Paleozoic section; whereas carbonate rocks with subordinate amounts of shale and clastic rocks predominate in the remainder. Some of the rocks, especially the Tintic Quartzite and some shales, are commonly limonitic, an important factor in analysis of Landsat MSS images. The volcanic rocks, mainly tuffs, flows, and agglomerates of quartz latitic and latitic composition, are limonitic in a few places where hematite is present in the groundmass.

Emplacement of monzonite and biotite monzonite porphyry bodies resulted in several types of altered rocks. Most widespread are argillized and silicified rocks, which are commonly bleached and limonitic. Locally, the intrusive rocks are also altered. Hydrothermal dolomite is common in the northern part of the area, and in the East Tintic mining district, calcitic, chloritic, and weakly argillized volcanic rocks and pebble dikes are widespread. Volcanic rocks subjected to an

early phase of "intravolcanic weathering" in this district are weakly altered but commonly limonitic. Barren as well as mineralized veins are present throughout the study area.

In situ spectral reflectance curves representing the most abundant altered and unaltered rocks show that the argillized and silicified rocks generally have intense ferric-iron and hydroxyl absorption bands owing to the presence of iron-oxide and hydroxyl-bearing phases, respectively. These features are generally absent in the unaltered rocks, except the limonitic rocks, which have prominent iron absorption bands. Both spectral features are weakly expressed in the volcanic rocks subjected to accelerated weathering. On the other hand, hydrothermal dolomite and calcitic volcanic rocks generally lack both features, and thus are spectrally similar to the unaltered rocks. Chloritic rocks are of limited distribution and have not been measured spectrally.

Most of the silicified and argillized areas are apparent in Skylab S190B, high altitude, and low altitude color aerial photographs because of the high albedo of these rocks. However, many unaltered rocks have similar albedos and therefore are not distinguishable from the altered rocks. Moreover, very little color information is available in these photographs. These problems are further complicated by brightness variations related to topographic slope.

MSS ratio images were generated to subdue the effects of topographic slope and albedo, and combined into several color composite images for displaying the spectral reflectance differences between the most widespread altered and unaltered rocks. The most effective combination

proved to be MSS 4/5, MSS 4/6, and MSS 6/7 using blue, yellow and magenta diazo films, respectively, rather than the MSS 4/5, MSS 5/6, and MSS 6/7 combination used so successfully in south-central Nevada. Consideration of schematic frequency distributions of ratio values for these two areas suggests that the lack of enhancement of limonitic rocks in MSS 5/6 images of the present study area is due to the higher frequency of low ratios representing vegetation.

Comparison of a limonitic bedrock map produced by scanning the optimum color-ratio composite image with a map of the silicified rocks shows good agreement, except where they are obscured by vegetation. Measurements of vegetation density indicate that shrub cover and juniper, pinyon, and sage cover greater than 40-50 and 33-43 percent, respectively, obscure limonitic rocks in these images. Argillized rocks, the most widely distributed altered rock type, were consistently detected in exposed areas. On the other hand, hydrothermal dolomite and calcitic and chloritic volcanic rocks are not portrayed in the limonitic bedrock map because of their general lack of limonite. Some altered rocks, especially veins and pebble dikes, are too small to be detected by the MSS except where they are closely spaced and well exposed.

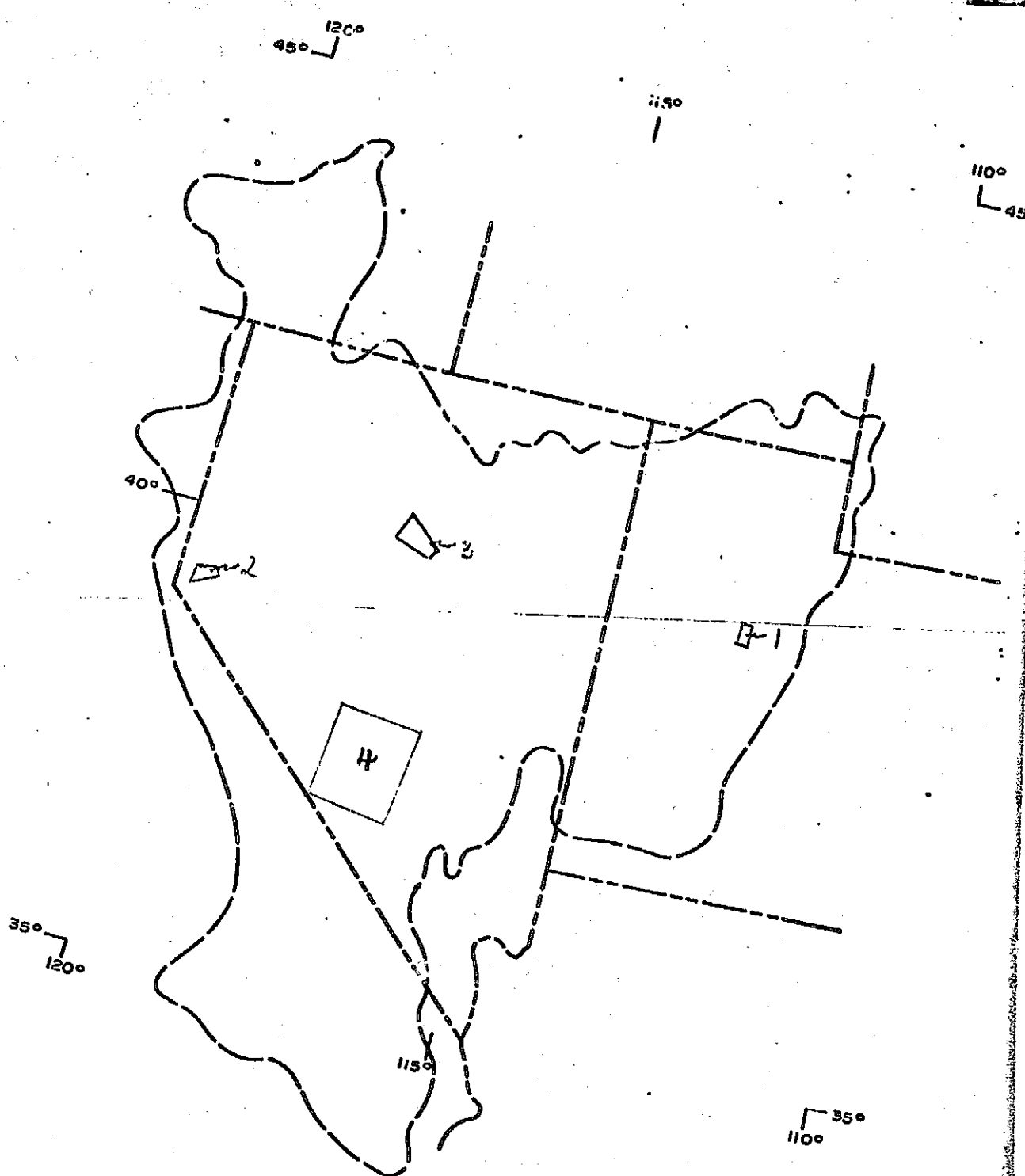
Another important limitation is that exposures of unaltered limonitic sedimentary and volcanic rocks are included in the limonitic bedrock map. Analysis of in situ spectral reflectance measurements indicates that this limitation can be largely overcome by obtaining radiance information in the 2.2 and 1.6  $\mu\text{m}$  regions.

## Introduction

The East Tintic Mountains are a generally north-trending block faulted range in central Utah near the eastern margin of the Great Basin (fig. 1). Approximately 30,000 feet of marine sediments of late Precambrian to Permian age are asymmetrically folded and transected by several different types of faults. These rocks, mainly carbonate, are partly overlain by Oligocene and Miocene volcanic rocks, including tuffs, agglomerates, and extensive latitic, quartz latitic, and trachy-andesitic flows. Dikes, sills, and small stocks of monzonite, quartz monzonite, and latite porphyry intrude all of the volcanic series. Hydrothermal alteration associated chiefly with the Oligocene volcanic activity has affected many of these rocks. Most of the ores of the three main mining districts, the Tintic, East Tintic, and North Tintic, occur as lead-zinc-silver replacement bodies in calcareous rocks and pyritic-copper-gold vein deposits in quartzite and the monzonite porphyry.

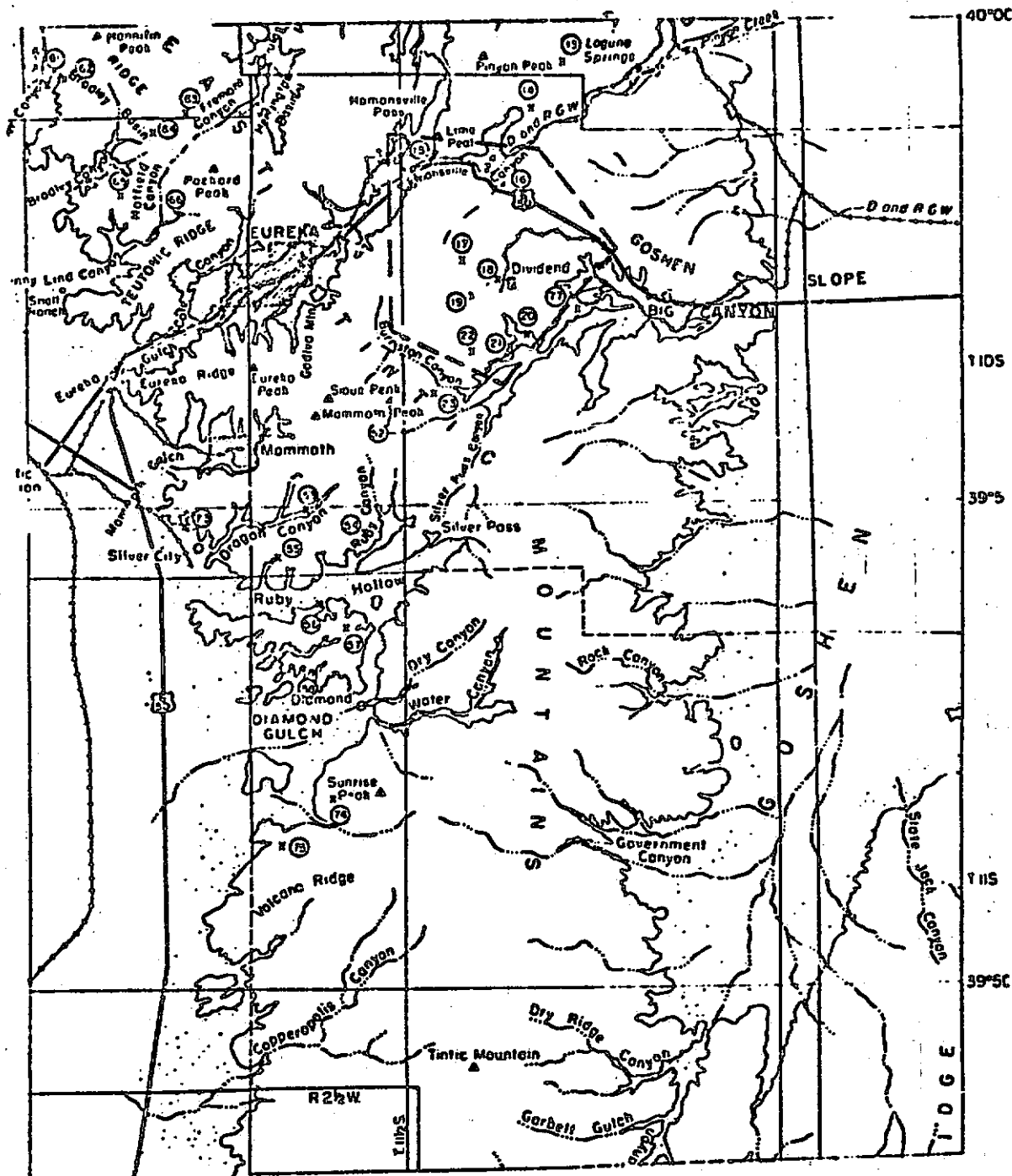
The central part of the East Tintic Mountains (fig. 2) was selected as one of three areas for further evaluation of the color-ratio composite (CRC) technique developed by Rowan and others (1974) for mapping limonitic hydrothermally altered rocks in the Goldfield region in south-central Nevada. The other areas studied during this Landsat follow-on experiment (ID No. 23890) are the Virginia Range southeast of Reno, Nevada, and the northwestern part of the Battle Mountain-Eureka mineral belt.

Figure 1 - Index map of the Great Basin showing locations of study areas: 1, East Tintic Mountains, Utah; 2, Virginia Range, Nevada; 3, Battle Mountain-Eureka mineral belt; 4, south-central Nevada.



ORIGINAL PAGE IS  
OF POOR QUALITY

1A-2



- |   |                                     |
|---|-------------------------------------|
| Eureka quadrangle                       | 47 Lower Mammoth mine               |
| 13 North Standard mine                  | 48 Gold Chert & ass shaft (lower)   |
| 14 Water Lily mine                      | 49 Ophelia mine                     |
| 15 Chief limestone quarry               | 50 Santa Catalina mine (No 1 shaft) |
| 16 Copper Leaf mine                     | 51 Iron Horse mine (No 1 shaft)     |
| 17 North Lily mine                      | 52 Crown Point mine (No 1 shaft)    |
| 18 Tintic Standard mine (No 2 shaft)    | 53 Dragon mine                      |
| 19 Eureka Lily mine                     | 54 A. L. mine                       |
| 20 Apex Standard mine (No 2 shaft)      | 55 S. L. mine                       |
| 21 Eureka Standard mine                 | 56 T. L. mine                       |
| 22 Iron King mine (No 1 shaft)          | 57 Shoshone mine                    |
| 23 Zuma mine                            | 58 Lark mine                        |
| 24 Raymond mine                         | 59 Hargis mine                      |
| 25 Colorado Chief mine                  |                                     |
| 26 Gemini mine                          | Tintic Mountain quadrangle          |
| 27 Bullion Rock mine                    | 59 Bullion mine                     |
| 28 Chief Consolidated mine (No 1 shaft) | 60 Tintic mine                      |
| 29 Plutus mine (Tintic shaft)           | 61 Van Wagon project                |
| 30 Eureka Hill mine                     | 62 Wagon project                    |
| 31 Central Eureka mine                  | 63 Field project                    |
| 32 Eagle and Blue Hill mine             | 64 Radio mine                       |
| 33 Victoria mine                        | 65 Victoria mine                    |
| 34 Cedar mine (shaft)                   | 66 North Rock mine                  |
| 35 May Day mine (shaft)                 | 67 Dugout mine                      |
| 36 Yankee mine (shaft)                  | 68 Black Warrior project            |
| 37 Humphrey tunnel                      | 69 Santa Fe mine                    |
| 38 Rock Tunnel mine (No 2 shaft)        | 70 Gandy quarry                     |
| 39 Saltator and Utah mine               | 71 Lark mine                        |
| 40 Colorado mine (No 1 shaft)           | 72 Golden Sunset mine (shaft)       |
| 41 Rocker shaft                         | 73 Santa Fe mine                    |
| 42 Over mine                            |                                     |
| 43 Grand Central mine                   | Tintic Mountain quadrangle          |
| 44 Iron mine                            | 74 Ruby mine                        |
| 45 Santa Ana tunnel                     | 75 Old Sun mine                     |
| 46 Mammoth mine (shaft)                 | 76 Tintic Chief project             |

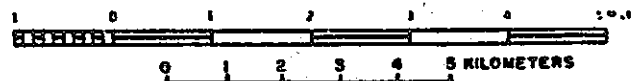
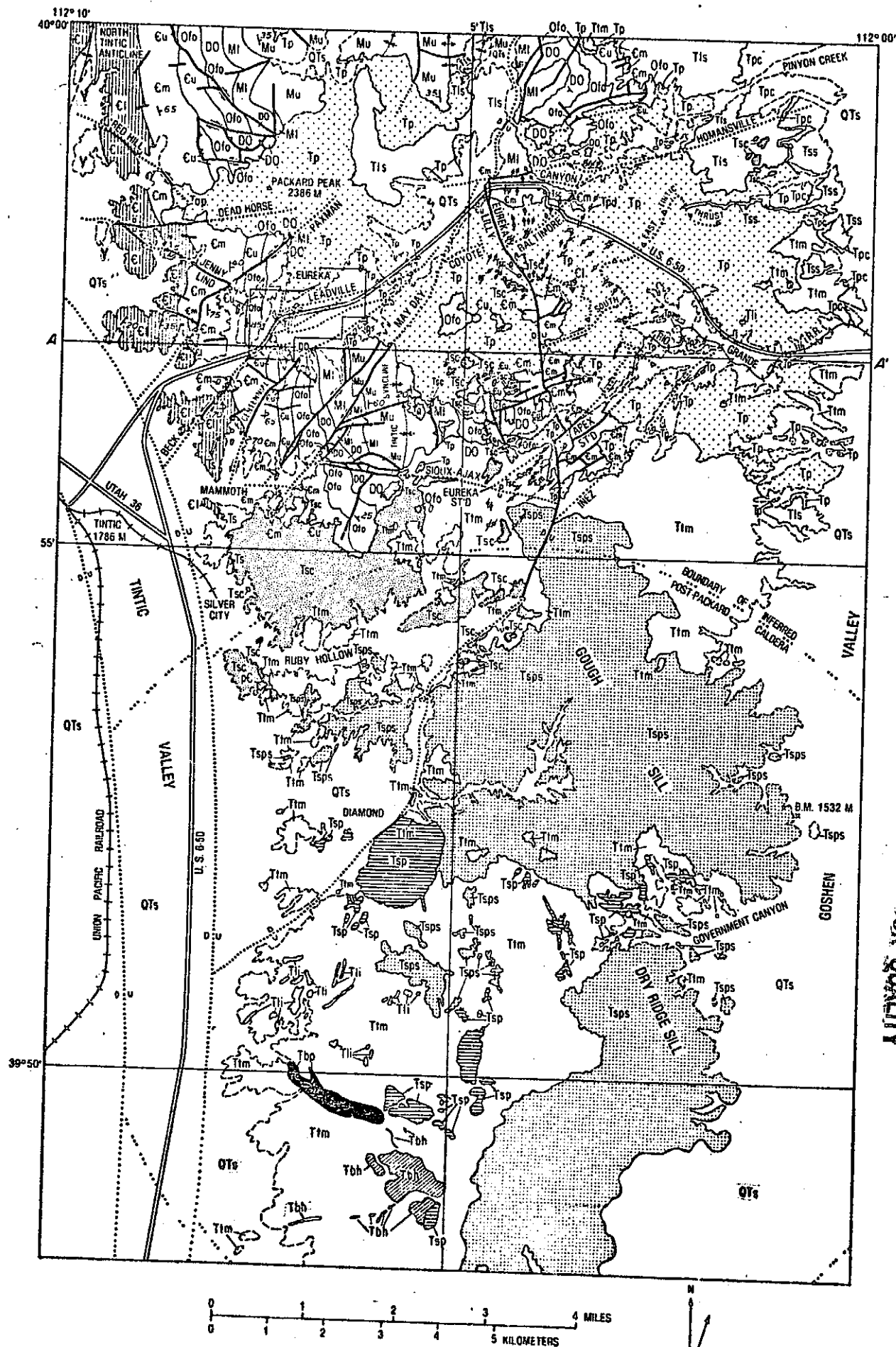


Figure 2 - Index map of the central part of the East Tintic Mountains study area showing locations of cultural and topographic features, mines and prospects, and the East Tintic mining district (dashed line).

which includes Battle Mountain and the Shoshone Ranges in north-central Nevada (fig. 1). In addition, detailed studies have continued in the part of south-central Nevada previously evaluated by Rowan and others (1977). The overall objective of this Landsat Follow-on experiment was to determine the effects of several geologic and environmental factors on the ability to discriminate hydrothermally altered rocks in Landsat Mss images. The most important factors are the mineral content and spectral reflectance of the altered rocks and host rocks, type, areal density and spectral reflectance of vegetation, size of altered areas, and topographic configuration.

The East Tintic Mountains provide an opportunity to examine a host rock assemblage that is substantially different from the dominantly volcanic rocks of south-central Nevada and the Virginia Range, and the siliceous, commonly ferruginous sedimentary rocks of the Battle Mountain and Shoshone Ranges. In addition, the alteration products in the East Tintic Mountains include types, such as calcitized flow rocks and hydrothermal dolomite, that are not present in the other areas, as well as argillized and silicified igneous and sedimentary rocks, which are common in the other study areas. Another important factor in the selection of this area is the presence of denser vegetation cover than is typical of most of the Basin and Range province.

The pre-Tertiary stratigraphy of the East Tintic Mountains has been described in detail by Lindgren and Loughlin (1919), Morris (1957), and Morris and Lovering (1961), and the central part of the range is covered by 1:24,000 scale geologic maps of the Eureka quadrangle



EXPLANATION	TERTIARY AND QUATERNARY
<div>QTs</div> <p>Surficial and valley-fill deposits</p>	
<div>Tss</div> <p>Silver Shield Quartz Latite and related feeder dike</p>	
<div>Tpc</div> <p>Pinyon Creek Conglomerate</p>	
<div>o--Tbp</div> <p>Breccia pipe</p>	
<div>Tsc</div> <p>Monzonite porphyry of Silver City stock and related plutons</p>	
<div>▧ Tpb ▧</div> <p>Pebble dikes and related dikes of monzonite porphyry</p>	
<div>Tls</div> <p>Laguna Springs Volcanic Group (Tintic Delmar Latite, Pinyon Queen Latite, and North Standard Latite)</p>	
<div>▧ Tsp Tsp</div> <p>Sunrise Peak Monzonite Porphyry and related intrusive rocks Tsp, crosscutting plutons Tsp, extensive sills</p>	
<div>Tli</div> <p>Latite intrusive rocks</p>	
<div>Ttm</div> <p>Tintic Mountain Volcanic Group (Big Canyon Latite, Latite Ridge Latite, and Copperopolis Latite)</p>	
<div>Ts</div> <p>Swansea Quartz Monzonite and related intrusive rocks</p>	
<div>Tp</div> <p>Packard Quartz Latite</p>	
<div>Tap</div> <p>Apex Conglomerate</p>	
<div>Mu</div> <p>Upper Mississippian rocks (Great Blue Formation, Humbug Formation, and Deseret Limestone)</p>	
<div>MI</div> <p>Mostly Lower Mississippian rocks (Gardison Limestone and Fitchville Formation; Includes some Devonian strata at base)</p>	MISSISSIPPIAN

<div>DO</div> <p>Devonian to Ordovician rocks (Pinyon Peak Limestone, Victoria Formation, and Bluebell Dolomite)</p>	ORDOVICIAN TO DEVONIAN
<div>Ofo</div> <p>Ordovician rocks (Fish Haven Dolomite and Opohonga Limestone)</p>	ORDOVICIAN
<div>Cu</div> <p>Upper Cambrian rocks (Ajax Dolomite and Opex Formation)</p>	
<div>Em</div> <p>Middle Cambrian rocks (Cole Canyon Dolomite, Bluebird Dolomite, Herkimer Limestone, Dagmar Dolomite, Teutonic Limestone, and Ophir Formation)</p>	CAMBRIAN
<div>Cl</div> <p>Lower Cambrian rocks (Tintic Quartzite)</p>	
<div>Y</div> <p>Big Cottonwood Formation</p>	PRECAMBRIAN
<p>-----</p> <p>Contact Dashed where approximately located</p>	
<p> </p> <p>Fault (Dotted where concealed; U, upthrown side; D, downthrown side; arrows show direction of relative movement. In section: A, relative movement away from observer; T, toward observer)</p>	
<p> </p> <p>Thrust fault (Dotted where concealed; Sawteeth on side of upper plate)</p>	
<p> </p> <p>Syncline (Showing trace of axial plane and plunge of axis)</p>	
<p> </p> <p>Anticline (Showing trace of axial plane and plunge of axis)</p>	
<p> </p> <p>Strike and dip of beds</p>	
<p> </p> <p>Strike and dip of overturned beds</p>	

**Figure 3 - Generalized geologic map of the study area (after Morris  
and Mogensen, 1978).**

(Morris, 1964a), the Tintic Junction quadrangle (Morris, 1964b), and the Tintic Mountain quadrangle and the adjacent part of the McIntyre quadrangle (Morris, 1975). This discussion draws extensively from these works for lithologic descriptions of the sedimentary and igneous host rocks; however, because of the low spatial resolution of the MSS images, reference is made mainly to the generalized 100,000 scale geologic map of the study area and a composite columnar section shown in figure 3 and table 1, respectively (from Morris and Mogensen, 1978). A more detailed analysis is presented for the East Tintic mining district, however, because of the presence of a large variety of hydrothermal alteration products (Lovering, 1949).

Particular attention is given to variations in surficial limonite content because of the common association of limonite with oxidized sulfide-bearing altered rocks and its diagnostic spectral reflectance in the MSS response range (Rowan and others, 1974; 1977). As used here, limonite consists mainly of hydrous iron-oxide minerals. Goethite is commonly dominant, but hematite and jarosite are also present; the individual mineral names are used where the components can be readily identified in the field. Spectral reflectance features at longer wavelengths are also considered, as these features may provide a basis for overcoming some of the limitations imposed by the MSS. No attempt has been made to evaluate the MSS images for structural information, even though north to north-northeast-trending faults were important in localizing ore minerals (Morris and Lovering, 1961) and some faults are quite apparent in the images.

### Acknowledgments

This Landsat Follow-on experiment (ID No. 23890) was partially supported by the National Aeronautics and Space Administration under contract number S-53953A. Hal Morris and Gary Raines, U.S. Geological Survey, made numerous helpful suggestions for improving the initial manuscript. We are also indebted to Helen Paley, Daryl Madura, and Danny Arias, Jet Propulsion Laboratory, Pasadena, California for the assistance in image processing and collection of field data.

## Lithology

### Sedimentary Rocks

Precambrian and Paleozoic sedimentary rocks are widespread in the northern one-third of the study area (fig. 3), whereas Tertiary volcanic and related intrusive rocks dominate the remainder. The most complete Paleozoic sections are exposed south and west of Eureka, Utah (fig. 3) in nearly vertical beds in the west limb of the overturned Tintic syncline. Although Precambrian to Permian rocks are present elsewhere in the East Tintic Mountains, Permian and Pennsylvanian rocks have been removed by erosion within the study area. As table 1 shows, the lower one-third of the composite section is dominated by clastic sediments. Carbonate rocks constitute most of the upper two-thirds, but arenaceous beds are common in some of the Devonian and Mississippian formations, and argillaceous layers are present throughout this part of the section.

Several map units are noteworthy because they include rocks characterized by prominent iron-oxide stains on weathered surfaces. The most widespread, well-exposed iron-oxide stained Paleozoic unit is the Tintic Quartzite (unit G2, fig. 3 and table 1). Tan, white, light pink, and gray, medium-grained, vitreous quartzites constitute the upper two-thirds of the section, but quartzite interlayered with hematitic quartzite grit and conglomerate are common in the lower part. The hematite occurs as coatings on grains and as a component of the cement. These layers are dark red to purple and weather to dark limonitic soil and

debris. Clastic white mica, rounded zircon grains, rutile, tourmaline, and sphene are common accessory minerals. The mica is important here because it commonly coats exposed bedding surfaces.

Another source of limonite in the Tintic Quartzite is oxidation of locally abundant disseminated pyrite. According to Morris and Lovering (1961), the pyrite is of hydrothermal origin and develops along joints and bedding planes of massive rock, as well as in breccia zones. Near mineralized fissures, brecciated quartzite is locally kaolinized, sericitized, or alunitized. Weathering of the pyritized quartzite results in rusty brown outcrops and soil.

Limonitic sedimentary rocks occur both above and below the Tintic Quartzite, but exposures are not as widespread. Below are gray-green pyllitic shale and greenish-brown vitreous quartzite of the Big Cottonwood Formation (unit Y, fig. 3 and table 1). The shale forms platy outcrops and shows little color change upon weathering. In contrast, the quartzite weathers to rust brown, apparently due to oxidation of an iron-carbonate mineral, as no pyrite has been reported (Morris and Lovering, 1961). Outcrops of the Big Cottonwood Formation are restricted to low hills in the northwestern part of the area.

Above the Tintic Quartzite, light to dark ocherous brown weathering shale of the Ophir Formation (unit 6m, fig. 3, and unit 6o, table 1) litters some gentle slopes. The most extensive series of outcrops are northwest of Eureka (fig. 3), but exposures are sparse elsewhere.

Yellowish and locally pink to red argillaceous material is also common in the Teutonic and Herkimer Limestones (part of unit Em, fig. 3, and units Ete and Eh, table 1), the Opex Formation (part of unit Eu, fig. 3, and unit Eop, table 1), and the Opohonga Limestone (part of unit Ofo, fig. 3, and unit Oop, table 1). In most places, the argillaceous material occurs as narrow seams of bands, and limestone is the dominant rock type, but locally, limonitic argillaceous rocks are prominent and impart conspicuous ocherous colors to the platy outcrops.

The remainder of the Paleozoic section consists mainly of limestone and dolomite, but the Deseret, Humbug, and Great Blue Formations (unit Mu, fig. 3, and units Md, Mh, and Mgb, table 1) contain iron-stained clastic beds that range from light and rust brown to pink, dusky red, and in the Deseret phosphatic beds, orange. The best exposures of these rocks are in the northwestern part of the study area (fig. 3).

The Apex Conglomerate (Oligocene) (unit Tap, fig. 3 and table 1) was deposited on a rugged surface carved into the Paleozoic and Precambrian units. The Apex Conglomerate has a highly variable composition and thickness. In general, it is composed of angular to rounded fragments of quartzite and subordinate shale and limestone in an indurated bright red sandy calcareous matrix (Morris and Lovering, 1961).

Volcanic rock fragments are absent. Although the Apex Conglomerate is important owing to its oxidized iron, exposures are generally poor, the best outcrops being west of Packard Peak in the vicinity of the Victoria Northwest mine (65, fig. 2) (Morris, 1964b).

Quaternary sedimentary deposits in the study area are mainly pediment gravels or fans along the range front and terraces and stream deposits in canyons. Locally, colluvium, chiefly talus and landslide debris, cover large areas. Lacustrine deposits of Lake Bonneville age are widespread in the basins, but these areas are beyond the limits of the study area.

The alluvial deposits are heterogeneous with respect to size, shape, bedding, sorting, cementation, and composition; however, iron and perhaps manganese-oxide stains and coatings are common on the exposed surfaces. In addition, some alluvial deposits are limonite stained where they overlie pyritized volcanic rocks. Thus, alluvial deposits constitute a significant problem in limonitic alteration mapping and must be distinguished from limonitic bedrock on the basis of morphologic differences.

### Igneous Rocks

Igneous rocks in the East Tintic Mountains represent the deeply eroded remnants of a composite volcano formed during early Tertiary time (Morris and Lovering, 1961). Volcanic activity began in middle Oligocene time, with catastrophic eruptions of the Packard and Fernow quartz latitic lapilli tuffs, massive welded tuffs, and near the sources, massive flows (unit Tp, fig. 3 and table 1).

The Packard Quartz Latite, named by Tower and Smith (1899) for extensive exposures at Packard Peak (fig. 3), and the Fernow Quartz Latite, named for exposures in the Ferner Valley south of the study area in the southern part of the East Tintic Mountains (Tower and Smith, 1899), appear to be parts of the same volcanic series separated by a region where younger latitic rocks overlie the quartz latite (Morris, 1957). The Packard is subdivided into four units: (1) a basal tuff; (2) a lower vitrophyre; (3) a massive flow unit; and (4) an upper vitrophyre (Morris, 1957). The thickness of the tuff ranges from a few centimeters up to 30 m, but is absent in many places.

The lower vitrophyre is chiefly black obsidian containing phenocrysts of biotite, sanidine, and quartz. Divitrification due to hydrothermal alteration has produced a rock that resembles fine-grained quartz latite. The thickness of the lower vitrophyre ranges from a few centimeters to 200 m, but it is locally absent.

The massive flow unit that caps large areas in the northern part of the range consists of medium-grained to dense quartz latite in which flow banding is commonly apparent. Phenocrysts of andesine, sanidine, quartz, and biotite make up 20 to 50 percent of volume (Morris, 1957). Although andesine and sanidine generally are present in equal proportions, andesine is locally dominant. Hornblende is present in some flows, but it is never abundant. Magnetite, apatite, sphene, and zircon are common accessory minerals.

On fresh surfaces, the color of the flow rocks ranges from light blue-gray to purplish-gray, but weathered surfaces are commonly rust brown due to oxidation of magnetite or the ferromagnesium minerals. Where the flows are very dense, a patchy black coating of desert varnish material is present.

Because the basal tuff and lower vitrophyre only partly smoothed out the rugged topography developed during the Permian to Oligocene hiatus (table 1), the thickness of the flow unit is highly variable. Morris (1957) reports that "in the east-central part of the Eureka quadrangle, a wedge-shaped mass of essentially homogeneous Packard

quartz latite fills a pre-lava valley that was more than 2700 feet deep" (Morris and Anderson, 1962). In a few places, presumably on pre-existing topographic highs, the unit is only a few hundred meters thick. Nevertheless, the quartz latite flow unit is one of the most widespread, best exposed, and most commonly altered units in the study area and therefore is especially important in this study.

The upper vitrophyre is similar to the lower vitrophyre, except that it is agglomeratic near the top and contains a few beds of fine- to medium-grained tuff (Morris, 1957).

The Fernow Quartz Latite, which is exposed south of the southern boundary of the study area, consists of a fine-grained to coarsely-fragmental basal tuff that commonly grades into an overlying vitrophyre or porphyritic quartz latite lava. The vitrophyre contains quartz, sanidine, and some biotite phenocrysts and is medium to pinkish-gray. The Fernow and Packard lavas have an aphanitic groundmass, but glassy streaks resembling collapsed pumice lapilli are common, indicating that much of these units may be welded tuffs rather than flows (Morris, 1957).

The Swansea Quartz Monzonite stock and a few dikes (unit Ts, fig. 3 and table 1) exposed south-southwest of Mammoth appear to be the intrusive equivalents of the Packard and Fernow Quartz Latites. Quartz, sodic andesine, orthoclase, biotite, and hornblende are the primary minerals. Common accessory minerals are magnetite, apatite, and zircon. The texture varies from granitic to porphyritic. Although the stock is

only about 1.2 km long and 0.5 km wide, it is important to this study because hydrothermal alteration results in a color change from pale grayish-pink to gray-green or light brown to white rock (Morris, 1957). The largest dike transects the Tintic Quartzite near the crest of Quartzite Ridge. Although it is extensively altered, the area of exposure is smaller than a Landsat picture element ( $\approx 79$  m).

Collapse after the eruption of the Packard Quartz Latite forming a caldera about 13.6 km in diameter centered 8 km southeast of Sunrise Peak (fig. 3) is inferred by Morris (1975) from the distribution of the quartz latite and older sedimentary rocks and the presence of a large positive magnetic anomaly (Mabey and Morris, 1967). Although the caldera was about 900 m deep, it was buried by the products of a second episode of volcanism. The initial deposits consisted of tuff, agglomerate, and spatter breccia which formed a cone 90-150 m high centered near Volcano Ridge in the southwestern part of figure 3. Superimposed on these rocks are air-fall tuff, dark gray lava flows, and agglomerates that completely filled the caldera.

The volcanic rocks of this second eruptive episode are referred to by Morris and Lovering (in press) as the Tintic Mountain Volcanic Group (unit Ttm, fig. 3 and table 1). The Tintic Mountain Volcanic Group consists of three formations: the Copperopolis Latite, the Latite Ridge Latite, and the Big Canyon Latite. These volcanic units are distinguished from the Packard Quartz Latite in containing abundant

augite and hypensthene, in addition to biotite, and only rare quartz phenocrysts. Sanidine and calcic andesine or sodic labradorite constitute the other major minerals of the rocks.

The Copperopolis Latite, which underlies extensive areas south and southeast of Diamond, consists of at least six members, four of which are in the area covered by figure 3. The lower agglomerate is a dark greenish-gray spatter breccia that contains lenses of lapilli and boulder tuff, and a few thin flows of dark gray latite.

The tuff member is chiefly a white to light green bedded air fall tuff, but in some places, such as south of Sunrise Peak (fig. 3), large areas are light pink or buff.

The lower flow member is widespread along the southwestern and southeastern flanks of the range. It consists of dark gray fine-grained porphyry with small phenocrysts of laboradorite, augite, and hypersthene. The groundmass is aphanitic to glassy.

Massive boulder agglomerate up to 1200 m thick makes up the middle agglomerate unit. The main components are rounded fragments of dark gray latite enclosed by a matrix of volcanic gravel and reworked tuff (Morris, 1975). In adjacent areas to the northeast and southeast, this unit is overlain by dark gray latite flows and an extensive upper agglomerate member that also contains some rather thick flow units. Apparently, these rocks have been removed from the study area by erosion (Morris, 1975).

The Latite Ridge Latite is extensively exposed in the southern and eastern parts of the East Tintic mining district on both the northeast and southwest sides of U.S. Highway 6-50. It consists of a lower white air fall tuff member and an upper reddish-brown fine-grained welded tuff member. Both of these members have been extensively altered by hydrothermal solutions in the southwestern part of the district.

The Big Canyon Latite is a relatively thin unit that overlies the Latite Ridge Latite north and south of Highway 6-50 near the eastern border of figure 3. It consists of a lower white air fall tuff and an upper flow unit of dark gray to black fine-grained latite porphyry. It is unaltered.

The intrusive equivalents of the Tintic Mountain Volcanic Group are the Sunrise Peak Monzonite Porphyry (unit Tsp, fig. 3 and table 1). Like the formations of the Tintic Mountain Volcanic Group, these plutonic rocks contain abundant phenocrysts of orthoclase, andesine, biotite, augite, and hypersthene, and only rare phenocrysts of quartz (Morris and Mogensen, in press). The Sunrise Peak stock lies a short distance southeast of Diamond and the great sills of Sunrise Peak Monzonite Porphyry underlie extensive areas northeast, east, and southeast of the stock. Other small plutons, dikes, and sills crop out in the area of Government Canyon (fig. 3).

After a short period of erosion that stripped the upper part of the Tintic Mountain Volcanic Group, the formations of the Laguna Springs Volcanic Group (unit Tls, fig. 3 and table 1) were deposited in the

northern part of the main Tintic mining district north of Eureka, and in the northeastern and southeastern part of the East Tintic mining district (fig. 3). This volcanic group consists of the North Standard Latite, the Pinyon Queen Latite, and the Tintic Delmar Latite. These formations are all similar in containing a lower member of tuff and lapilli breccia and an upper member of coarsely porphyritic flow rock. The Laguna Springs lavas are characterized by containing phenocrysts of sodic andesine, sanidine, biotite, hornblende, and augite. Although the volume of the Laguna Springs eruptive rocks is relatively small as compared to the great volumes of the Packard Quartz Latite and the Tintic Mountain Volcanic Group, they are of substantial importance and interest inasmuch as their eruption was followed by the emplacement of the monzonite porphyry of the Silver City stock and its satellite plutons. The great floods of hydrothermal solutions that altered the rocks of the Tintic and East Tintic mining districts and deposited the extensive ore bodies were active during the final cooling stages of these intrusive bodies (Morris and Mogensen, in press).

The monzonite porphyry of the Silver City stock extends southward from Mammoth to Ruby Hollow (unit Tsc, fig. 3 and table 1). The monzonite porphyry is altered in many places, but fresh specimens are dominantly light gray with faint purplish, brownish, and pink variations. Andesine, orthoclase, quartz, hornblende, augite (commonly uralitized), biotite, magnetite, apatite, zircon, and sphene are the most common minerals. The texture varies within the body from medium to fine-grained granular in central and western parts to porphyritic in the eastern half.

A zone approximately 0.8-2.5 km wide of dominantly biotitic monzonite porphyry plugs, dikes, and small stocks extends northeast from the Silver City stock through the East Tintic mining district to the Homansville fault (part of unit Tsc, fig. 3 and Table 1). A narrower zone of monzonite porphyry dikes (part of unit Tpd, fig. 3 and Table 1) occurs within this zone southeast of the Homansville fault. These bodies appear to be contemporaneous with the Silver City stock (Morris, 1957), although they are distinctly more coarsely porphyritic and compositionally variable. Xenoliths of sedimentary rocks are common in some of these plugs and dikes, and some of the quartz phenocrysts appear to be rounded fragments of Tintic Quartzite. The color of fresh samples of the porphyry ranges from light to dark gray and locally pink, but alteration is widespread.

Another important rock type associated with this period of magmatic intrusion is the pebble dikes (part of unit Tpd, fig. 3 and Table 1) concentrated in the northern and eastern parts of the above described zone. These dike-like or lensoidal bodies consists mainly of abrasion-rounded quartzite pebbles in a matrix of pulverized quartz and carbonate material; shale and limestone fragments are present, but distinctly subordinate. Their dimensions range from a few centimeters to a meter or two in width and about a meter to several hundred meters in length. Exposures of pebble dikes locally consist only of a linear zone strewn with dark brown to nearly black limonitic pebbles. Some of these bodies

have been traced downward in mine workings into monzonite porphyry dikes, but others are apparently rootless (Morris, 1957). Lovering (1949) suggests that some of these bodies developed in drag zones on top of or along the edge of viscous monzonite bodies, whereas most of them are probably explosion breccias.

A compositionally similar but much larger body is present in the southern part of the study area along Copperopolis Canyon (unit Tbp, fig. 3 and table 1). Morris (1975) describes this body as a breccia pipe consisting of quartzite, shale, and limestone fragments in a matrix of shattered phenocrysts of quartz, sanidine, and plagioclase, and rock flour with disseminated pyrite. Oxidation of the pyrite has resulted in a medium to light brown limonite coating on the fragments. The fragments are larger and less rounded than in the pebble dikes, however.

The youngest igneous rocks in the central East Tintic Mountains are a wide dike and an associated flow unit of coarse-grained porphyritic quartz latite of Miocene age that crops out in the northeastern part of the East Tintic mining district north of U.S. Highway 6-50 (Morris and Lovering, in press). This unit is named the Silver Shield Quartz Latite (unit Tss, fig. 3 and table 1). It contains abundant large phenocrysts of quartz, sanidine, andesine, biotite, augite, and hypersthene. The flow unit overlies the Pinyon Creek Conglomerate (Miocene) (unit Tpc, fig. 3 and table 1), which is faintly pyritized, and adjacent to the dike are small to moderate-sized masses of opalized volcanic rocks.

### Hydrothermally Altered Rocks

Hydrothermal alteration associated with emplacement of the Oligocene intrusive rocks resulted in numerous stages of chloritized, argillized, pyritized, calcitized, and silicified igneous rocks, and dolomitized, sanded, pyritized, and silicified sedimentary rocks. The silicified areas (fig. 4), as compiled from the above-mentioned 1:24,000 scale geologic maps, are concentrated in the northern and central parts of the study area near the Swansea, Sunrise Peak, Silver City, and associated plutons. Most of the silicified areas are 200-300 m across, and none are larger than 2 km.

Argillized rocks are much more widespread than silicified rocks. However, argillized rocks have not been mapped except in the East Tintic mining district (fig. 2), and in one large area southeast of Copperopolis Creek.

Vein deposits are common in some areas, especially between Diamond Gulch and approximately 2.5 km south of Eureka (fig. 4). Some of these veins are mineralized, whereas others are barren. Another important type of small-scale intrusive feature is the above-described pebble dikes in the East Tintic mining district (fig. 2). Although the widths of individual veins and pebble dikes are well below the spatial resolution (79 m) of the MSS, closely spaced clusters or sets, a common occurrence, might be detectable. Also, the downslope washing of eroded debris locally makes the surface distribution of these veins much larger than the outcrop of the body.



Figure 4 - Map showing the distribution of moderately and intensely silicified rocks (dark), mineralized veins (solid lines), unmineralized veins (dotted lines), and pebble dikes (short dashed lines) in the study area (compiled from Morris, 1964a, b; 1975). Area southeast of Copperopolis Creek consists mainly of argillized latite and area to north is a quartzitic breccia (Morris, 1975).

Brief mineralogical descriptions are available for some of the silicified and altered areas in the study area, but the East Tintic mining district rocks have been studied in great detail by Lovering (1949) (fig. 5). Therefore, the remainder of this section is devoted to discussion of the mineralogy of the hydrothermally altered rocks of this district. This discussion provides the main basis for evaluation of in situ reflectance spectra and the MSS CRC image.

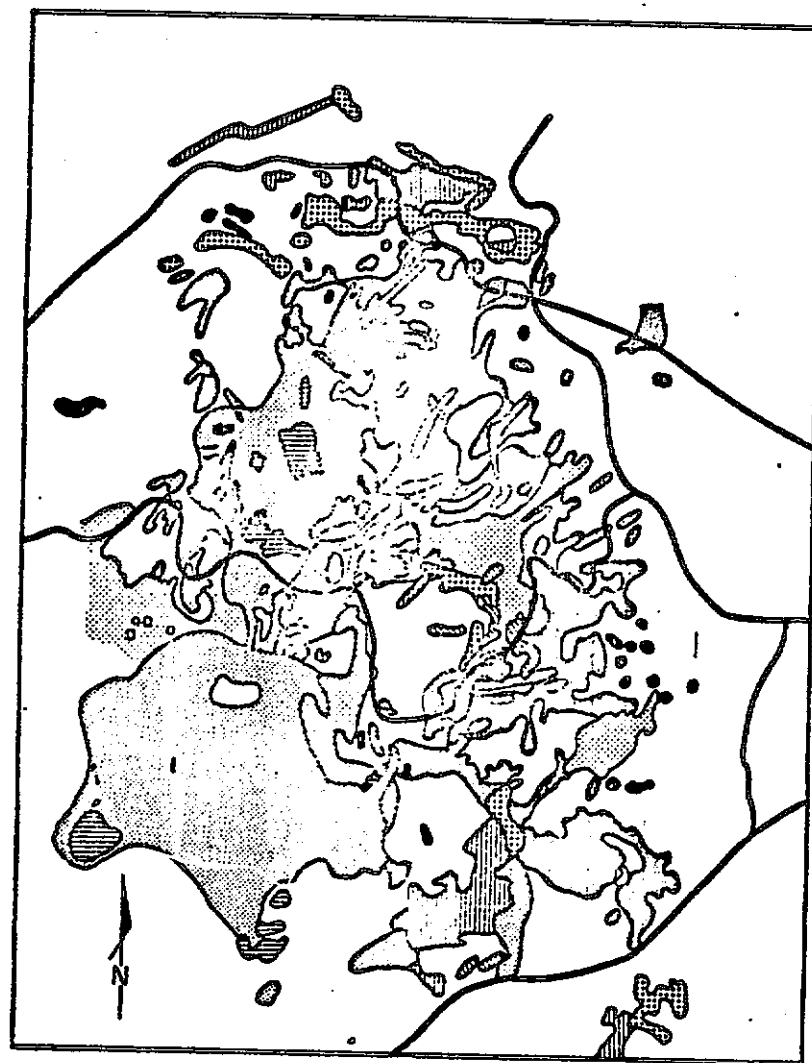
The Tintic mining district, which includes both the main Tintic and East Tintic "districts", has produced \$568,620,000 in metals to 1977, and is still active; it was the site of a series of hydrothermal events which Lovering (1949, p. 16) describes as follows:

"1. Early Barren Stage - widespread hydrothermal dolomitization of limestones and chloritization of the lower part of the overlying volcanics.

2. Mid-Barren Stage - widespread argillic alteration of the volcanic rocks near centers of intrusion, and localized argillic alteration of argillaceous sedimentary rocks and sanding and solution-brecciation of carbonate rocks. Characterized by the abundant development of clay minerals and much leaching, transportation, and reprecipitation of silica and the bases. Pyrite began to form in this stage, commonly in thin veinlets that make up less than one percent of the rocks.

3. Late Barren Stage - moderately extensive silicification of dolomite and limestone near centers of mineralization and some silicification of the overlying lavas: jasperoid (allophane-quartz), pyrite and barite, and the level of ore deposition, with pyrite, calcite, and allophane-quartz on the outlet side. Pyritization and coleitization of the lavas was also important during this stage.

30



# EXPLANATION


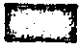






-  Replacement ore bodies
-  Silicified rocks
-  Calcitic volcanic rocks
-  Pyritized rocks
-  Argillized rocks
-  Chloritized volcanic rocks
-  Hydrothermal dolomite
-  Monzonite porphyry

Figure 5 - Alteration map of the East Tintic mining district  
(generalized from Lovering, 1949).

4. Early productive stage - potassic alteration (sericite and hydromica), clear quartz, barite, and pyrite.

5. Productive stage - ore sulfides and sulfosalts, pyrite, tellurides, gold, quartz, and carbonates."

In addition, Lovering describes an "intra-volcanic accelerated weathering" stage that may have been related to the introduction of hot neutral or mildly acidic bicarbonate water near steam vents rather than to weathering. The association of the main alteration minerals with these stages of alteration are shown in table 2.

According to Lovering (1949), the intra-volcanic accelerated weathering resulted in zones of downward flaring bleached quartz latite concentrated along major faults. The rock disintegrates easily, but the biotite and feldspar phenocrysts are generally unaltered or only partly converted to limonite and clay minerals, respectively (table 2). The groundmass is bleached and has been converted largely to allophane due to hydration. Although Lovering did not map the distribution of these rocks, we regard them as being weakly altered.

The distributions of the clearly hydrothermally altered rocks in the East Tintic mining district are shown in figure 5, a slightly generalized compilation of Lovering's three alteration maps that excludes pebble dikes, mineralized fissures in quartzite, small monzonite porphyry dikes, and structural information. Chloritized



Table 2 - Paragenesis of alteration and ore minerals in the East

Tintic mining district, Utah (from Lovering, 1949).

volcanic rocks and dolomitized limestones of the early barren stage occur together, except where the underlying rocks are highly fractured Tintic Quartzite (fig. 5). In the East Tintic mining district, the chloritized rocks are especially common in the lower part of the Packard Quartz Latite. Elsewhere in the study area, the chloritized volcanic rocks are rare and are largely restricted to areas near fractures. Chloritized quartz latite is characterized by its dark green color and the presence of chlorite seams, chlorite-quartz veins, and alteration of some ferromagnesium minerals to minerals of the chlorite group. Weathering commonly results in dark red-brown rocks consisting mainly of chlorite, heidellite, montmorillonite, allophane, and limonite. These rocks are considerably more friable than unaltered, weathered quartz latite.

Conversion of limestone to hydrothermal dolomite through intense leaching of CaO and the addition of MgO results in darker rocks where the limestone was originally medium to dark gray. Upon weathering, these rocks become still darker, probably due to an increase in manganese, iron, and carbonaceous material on the surface (Lovering, 1949). Light gray or white limestones tend to yield light tan hydrothermal dolomite.

Unlike chloritized volcanic rocks, hydrothermal dolomite is common in many parts of the study area. The most susceptible formations are the limestone member of the Ophir Formation, the Teutonic and Herkimer Limestones, and the Dagmar Dolomite, especially in areas where structural

adjustments had opened passageways for the dolomitizing fluids (Lovering, 1949; Morris and Lovering, 1961). In fact, Morris and Lovering suggest that the Bluebird Dolomite might be a hydrothermal dolomite instead of a primary dolomite, as it has been regarded by most workers, inasmuch as it is a limestone in outlying areas away from ore. The Opohonga Limestone also is commonly dolomitized near intrusive centers and along fault zones, even though it is not extensively fractured.

During the middle barren stage, large areas of volcanic rocks were intensely argillized, resulting in conspicuously bleached rocks with seams of yellow-brown limonite and jarosite. The spatial relationship between these rocks and the biotite-monzonite porphyry bodies is clear in the East Tintic mining district (fig. 5). In contrast with the chloritized lava, every mineral except phenocrystic quartz was attacked by the argillizing fluids, and chemical analyses show a net loss of all constituents except water above 110°C, which was added (Lovering, 1949).

Two stages of argillic alteration have been recognized (Lovering, 1949): (1) an early widespread pervasive diffuse argillization, and (2) a later, more localized and variable argillization associated with fractures and intrusive contacts with the volcanic rocks. The early argillization is characterized by a quartz-kaolinite assemblage where the volcanic rocks are intensely altered and by montmorillonite beidellite clays where the alteration is moderate. In general, the

phenocrysts are more susceptible than the more silicic and potassic groundmass, and the grain size of the clay minerals increases with increasing intensity of alteration (Lovering, 1949).

The later argillic rocks are commonly zones in the vicinity of the biotite monzonite porphyry bodies. In general, the sequence grades outward from sericitized, silicified quartz latite in the contact zone through alunitized rocks into a broader argillized zone, but local variations are common. The areal extent of these zones is rarely greater than about 100 m, approximately the size of an MSS pixel.

The intrusive rocks are also locally altered, especially adjacent to the zoned argillized quartz latite. Plagioclase, biotite, and hornblende phenocrysts are converted to kaolinite and dickite, and the groundmass is altered to kaolinite, beidellite, and potash clay or hydromica (Lovering, 1949). One of the largest argillized areas is an intensely argillized latite plug located southeast of Copperopolis Creek (fig. 4). These bleached rocks consist mainly of kaolinite and quartz, but contain unaltered sanidine and quartz phenocrysts (Morris, 1975).

Paleozoic sedimentary rocks were also argillized, but the areas are generally much smaller than the pervasively argillized volcanic rocks. The largest area is the Dragon mine, about 1.5 km southeast of Mammoth (fig. 2), where Ajax Dolomite and Opohonga Limestone have been replaced by halloysite and endellite in the contact zone with the monzonite porphyry of the Silver City stock. In the East Tintic mining district, only a few

pipe-like bodies of similar composition have been found, but extensive masses of sanded dolomite and solution breccia indicate reaction of the carbonate rocks with the strongly acidic solutions that are believed to have converted the aluminous igneous rocks to clay.

Late barren stage alteration is characterized by silicification and pyritization of both the sedimentary and volcanic rocks, and by widespread calcification of the volcanic rocks. The silicified rocks, referred to as jasperoids, consist mainly of fine-grained quartz, barite, some opal, rutile, and chlorite (Table 2). In the East Tintic mining district, these typically dark red-brown to dark gray vitreous and highly fractured rocks are commonly confined to areas 100 m across, and nowhere are the deposits larger than 200 m across (fig. 5); however, altered rocks of similar mineralogy but commonly higher albedo are widespread elsewhere in the study area (fig. 4).

Pyritic rocks of the late barren stage underlie larger areas of the central part of the East Tintic mining district (fig. 5), and are more conspicuous by virtue of the presence of abundant limonite and jarosite on exposed surfaces and along fractures. The pyritic volcanic rocks are also bleached, although not as intensely as the argillized rocks. Where pyrite was abundant, extensive cation leaching has taken place, but seldom was this secondary acid-solution attack as intense as it was during primary argillization.

A widespread alteration product of the late barren stage is calcitic volcanic rock (fig. 5); however, this rock is also the least conspicuous because the calcite replaces plagioclase phenocrysts, rarely affects the groundmass, and results in a light blue, slightly granular rock, which otherwise appears unaltered. In addition, the calcite has been leached from many exposed surfaces.

Calcitic alteration continued into the early productive stage, but the distinguishing feature of this stage is potassic alteration in the form of hydromica or, in intensely altered zones, sericite (table 2). Pyrite and clear quartz were also deposited in voids. The potassic alteration is restricted to envelopes or zones closely adjacent to ore bodies, and therefore involves small areas, generally 100-300 m across. In quartzite and generally in limestone, potassic alteration is concentrated in previously argillized zones, but shale, monzonite porphyry, and quartz latite were susceptible even where argillization is lacking. During the productive stage, quartz barite, pyrite, and rhodochrosite were the most common gangue minerals formed. Because of the presence of pyrite in the rocks of the early productive stage, weathering has produced conspicuous limonite stains, and in most places the rocks are bleached. Thus, their general appearance is similar to that of the argillic rocks of the middle barren stage and the pyritic rocks of the late barren stage.

## Vegetation

Vegetation in most of the East Tintic Mountains is typical of the Upper Sonoran Life Zone (Preston, 1968), but the Transition and Canadian Life Zones are represented at higher elevations. The alluvial basins and lower slopes of the range are characterized by sage (*Artemisia*) and lesser amounts of prickly pear (*Opuntia*), hedgehog (*Echinocereus*) and bunch grasses. Rabbit brush (*Chrysothamnys*) occurs where soil moisture is high. Pinyons and junipers are scattered throughout the alluvial fans.

As elevation increases, sage remains dominant, but pinyon pines (*P. monophylla* and *Pinus edulis*) and locally thick stands of Utah and mountain juniper (*Juniperus osteosperma* and *J. scopulorum*) are scattered along these intermediate slopes (Morris and Lovering, 1961). On sunny slopes, Brigham's tea (*Ephedra viridis*), curl-leaf mahogany (*Cercocarpus ledifolius*), antelope brush (*Purshia tridentata*), cliff rose (*Cowania neomexicana*), hackberry (*Celtis reticulata* and *C. douglasii*), and juneberry (*Amelanchier alnifolia*) are present. The availability of moisture in canyons, especially near springs, results in thickets of dwarf and big-tooth maples (*Acer glabrum* and *A. grandidentatum*), the latter being a representative of the Transition Life Zone. A few box elder (*Acer negundo*), cottonwood (*Populus angustifolia* and *P. acuminata*), barberry (*Berberis repens*), gooseberry (*Ribes inerme*), choke cherry (*Prunus melanocarpa*), mountain elder (*Alnus tenuifolia*), and hawthorn (*Crataegus* sp.) also occur in these areas (Morris and Lovering, 1961).

Species that represent the Canadian Life Zone are sparsely present at the highest elevations, including aspen (*Populus tremuloides*), yellow pine (*Pinus scopulorum*), Douglas fir (*Pseudotsuga taxifolia*), white fir (*Abies concolor*), and Englemann spruce (*Picea englemannii*). These trees grow preferentially, though not exclusively, on northward-facing slopes.

The areal density of vegetation in the East Tintic Mountains is highly variable, but it is substantially greater than the cover in south-central Nevada and along most of the Battle Mountain-Eureka mineral belt and is roughly comparable to most of the Virginia Range study area. Areal densities of the most widespread species, sage, juniper, and pinyon are influenced by several fairly obvious factors, such as altitude, temperature, and precipitation. A less obvious but very important factor is the effect of argillization. In some areas of argillized volcanic rocks, the density of sage decreases markedly, whereas the density of pinyon and juniper is not obviously changed. The explanation for this decline in shrub cover has not been determined in these areas, but Billings (1950) concluded that similar changes in the Virginia Range, Nevada area were the result of deficiencies in nitrogen, phosphorus, and perhaps magnesium. This possibility is being considered in a recently initiated study, along with increased clay content and more rapid erosion in the altered rocks and residual soils.

Large areas of the Tintic Valley (fig. 2) are part of an experimental program for eradicating sage and developing grass land. These areas are of interest here because they are conspicuous in the enhanced MSS images discussed later. Although spectral measurements are not available, the MSS ratio values clearly indicate concentrations of iron-oxide minerals on the surface, presumably due to accelerated oxidation of the disturbed soil and thin grass cover when the image was recorded.

## Spectral Reflectance

The visible and near-infrared (0.4-2.5  $\mu\text{m}$ ) spectral reflectance of rocks and soils are dominated by electronic processes and vibrational processes that take place in transitional metal anions and in anion groups, respectively (Hunt, 1977). These processes give rise to absorption bands, which can be used to discriminate some geologic materials in multispectral images and to place some bounds on the mineralogical composition. Identification in the classical petrologic sense is rarely possible, however.

Ferric and ferrous iron are the most common sources of electronic absorption bands in terrestrial rocks, although titanium, zinc, and manganese exhibit similar spectral features. The most intense ferric absorption bands occur in the ultraviolet, near 0.7  $\mu\text{m}$  and 0.9  $\mu\text{m}$ ; subordinate bands are centered at about 0.40  $\mu\text{m}$ , 0.45  $\mu\text{m}$ , and 0.49  $\mu\text{m}$  (Hunt and Salisbury, 1970). The major ferrous absorption band is located near 1.0  $\mu\text{m}$ , but minor bands are commonly present near 0.43  $\mu\text{m}$ , 0.45  $\mu\text{m}$ , 0.51  $\mu\text{m}$ , and 0.55  $\mu\text{m}$ . Also, iron-rich orthopyroxene has an intense ferrous band near 1.8  $\mu\text{m}$ .

The most intense vibrational absorption bands occur near 1.4  $\mu\text{m}$ , 1.8  $\mu\text{m}$ , 2.2  $\mu\text{m}$ , and 2.35  $\mu\text{m}$ . Although the 1.4 and 1.8  $\mu\text{m}$  bands are useful for analyzing laboratory spectra, atmospheric absorption by water precludes recording useful field spectra or images in these regions. The 2.2  $\mu\text{m}$  band is a combination of stretching and bending overtones related

to more intense features occurring in OH molecules at longer wavelengths (Hunt and Salisbury, 1970). This band is especially important for mapping altered rocks with hydroxyl-bearing minerals. The 2.35  $\mu\text{m}$  band is related to overtones occurring in the  $\text{CO}_3^{-2}$  molecule.

In situ reflectance measurements were collected in the East Tintic Mountains using the Jet Propulsion Laboratory portable field reflectance spectrometer (PFRS) (Goetz and others, 1975) to determine the main spectral changes resulting from alteration of the sedimentary and igneous rocks. However, because of unsuitable sky conditions, only 132 spectra were recorded, mainly for the fresh unaltered and altered quartz latitic rocks. Although these data are not adequate for a comprehensive discussion, representative spectra are useful for illustrating the most important changes caused by increasingly intense hydrothermal alteration of the Packard and Fernow Quartz Latites, the most widespread rock type. All of the spectra have been smoothed manually to remove minor variations due to instrument noise and atmospheric perturbations. Data is not plotted in the 1.4  $\mu\text{m}$  and 1.9  $\mu\text{m}$  regions due to the low noise signal in the areas of high atmospheric absorption.

The unaltered quartz latite flow rock is characterized by low albedo and gradually increasing reflectance in the MSS response region and essentially constant reflectance in the longer wavelength region (fig. 6a). This general shape, which is typical of rocks of similar composition in south-central Nevada (Rowan and others, 1977) is indicative of a silicate rock which has little limonite surface staining or hydroxyl-bearing minerals.

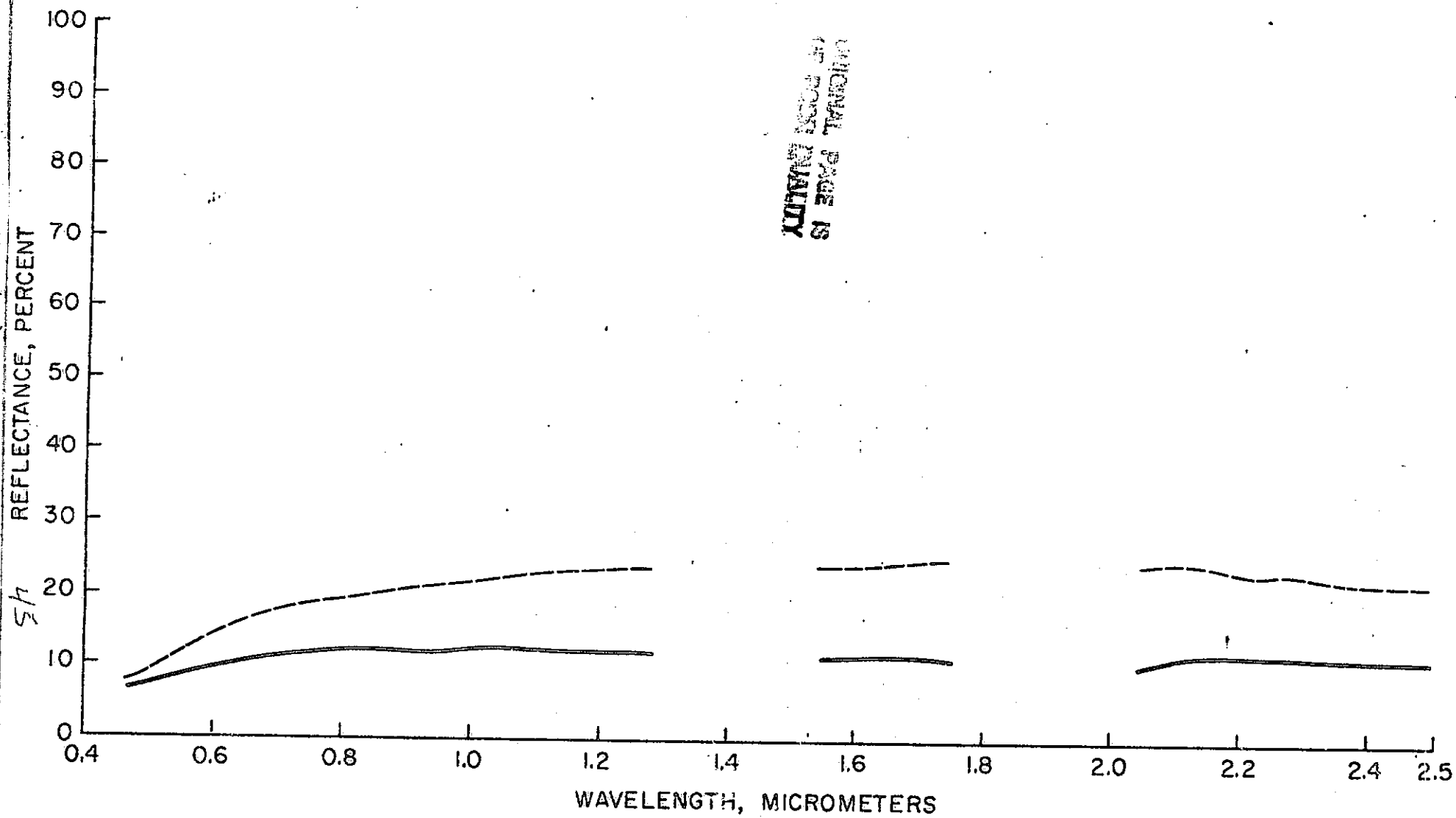


Figure 6 - Representative in situ reflectance spectra for (a) unaltered quartz latite flow rock (solid lines) and (b) weathered quartz latite flow rock and residual soil (dashed line).

Weathering of the quartz latite flow rock and formation of soil increases the albedo and intensifies the ferric absorption bands somewhat (fig. 6b), mainly because of conversion of ferromagnesium and opaque minerals to iron-oxide minerals and a general decrease in grain size conversion. In addition, a very weak hydroxyl band near 2.2  $\mu\text{m}$  suggests the presence of some clay, probably montmorillonite, in the soil. This soil appears to be chiefly a mechanical rather than chemical product of weathering and hence its low clay content.

Accelerated intravolcanic weathering of the packard Quartz Latite in the East Tintic mining district (Lovering, 1949) gives rise to more prominent spectral changes. In general, limonite and montmorillonite are more abundant in these rocks than in their weathered unaltered equivalents. Consequently, the ferric absorption bands near 0.90  $\mu\text{m}$  and the visible wavelength region and the 2.2  $\mu\text{m}$  hydroxyl band (fig. 7) are more conspicuous than in the unaltered rocks, even where soil is present (fig. 6b). Examination of 14 in situ spectra indicates that the range of the decrease in reflectance at 2.2  $\mu\text{m}$  relative to 1.6  $\mu\text{m}$  is about 15-20 percent, compared with less than 5 percent for the unaltered weathered quartz latite. In general, the rocks affected by intravolcanic weathering also have slightly higher albedos.

Calcitic quartz latite attributed to the late barren stage alteration (Lovering, 1949) is spectrally more variable than rocks affected by intravolcanic weathering. Based on analysis of 13 spectra collected at two sites in the East Tintic mining district, the typical

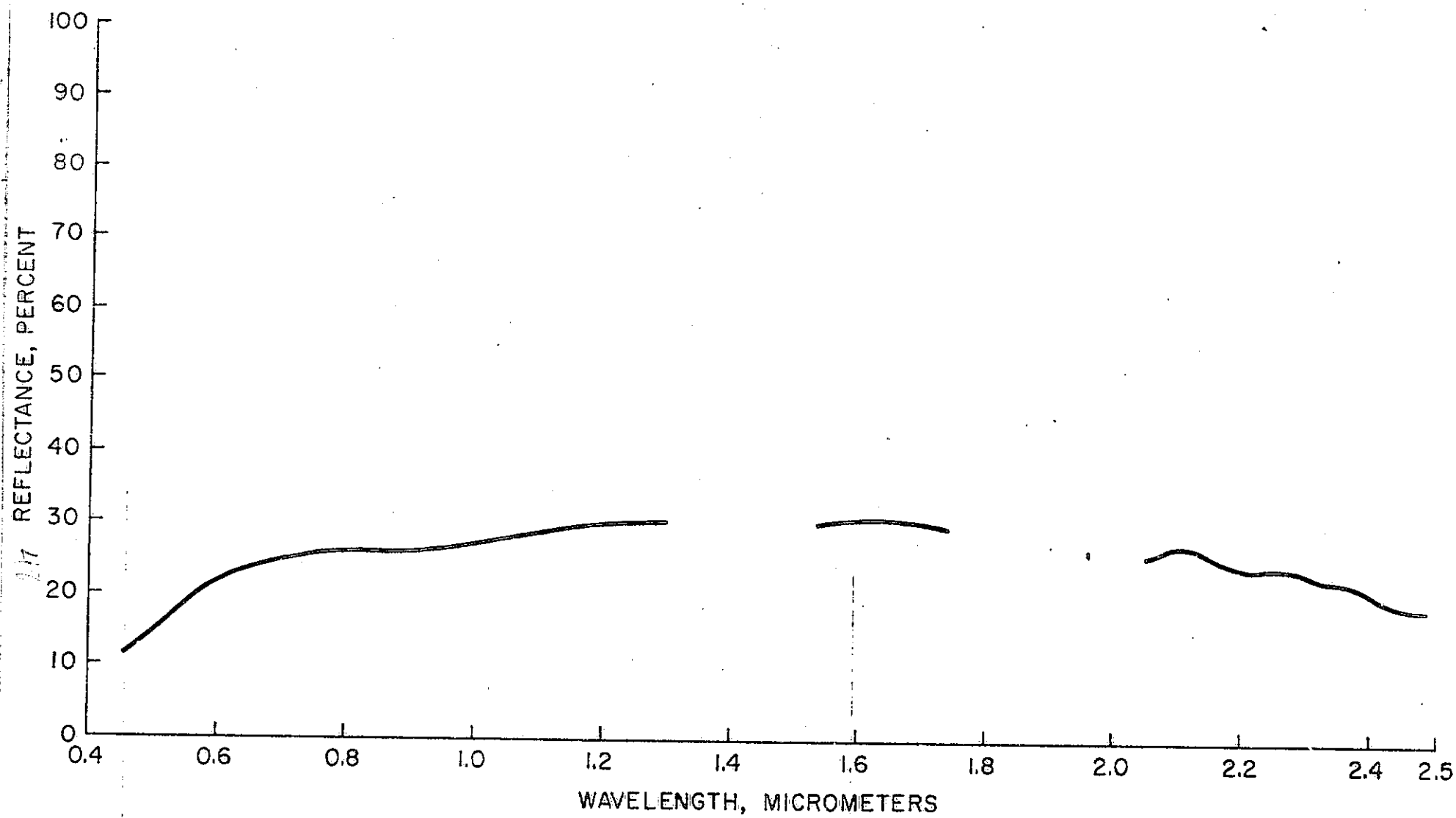


Figure 7 - Representative in situ reflectance spectrum for quartz  
latite flow rock subjected to accelerated weathering.

spectrum is characterized by very weak ferric absorption bands and gradually decreasing reflectance beyond about 1.3  $\mu\text{m}$  (fig. 8a). Locally, a very subtle band appears at 2.2  $\mu\text{m}$  due to the presence of montmorillonite (fig. 8b). The 2.35  $\mu\text{m}$  band that might be expected in rocks containing  $\text{CO}_3^{-2}$  molecules is not present in any of these spectra owing to leaching of the calcite from the exposed surface. In a few places, the ferric bands are more apparent (fig. 8c), and the spectrum is similar to weathered unaltered samples containing soil (fig. 6b).

In argillized volcanic and intrusive rocks, the increased abundance of limonite and, locally, jarosite, and of clay minerals causes more intense ferric and hydroxyl absorption bands than in the above described spectra. Representative in situ spectra for four argillized areas are shown in figures 9-12. Because the alteration map (fig. 4) shows only silicified zones, veins, and pebble dikes, none of these sample areas are shown in figure 4.

The Government Canyon altered area consists of latitic tuff of the Tintic Mountain Volcanic Group (unit Tfm, fig. 3 and table 1), which has been extensively intruded by Sunrise Peak Monzonite Porphyry dikes, sills, and plugs (units Tsp and Tsps, fig. 3 and table 1). Pyrite, typically 0.5-1.0 mm cubes, is widespread. In some places, the pyrite is reasonably unweathered, but elsewhere decomposition has yielded a prominent limonite coating. Large areas are bleached by the leaching action of acid solutions where the pyrite has decomposed. Ferric and hydroxyl absorption bands are well developed, with the 2.2  $\mu\text{m}$  reflectance being about 25-30 percent lower than the 1.6  $\mu\text{m}$  reflectance (fig. 9a, b).

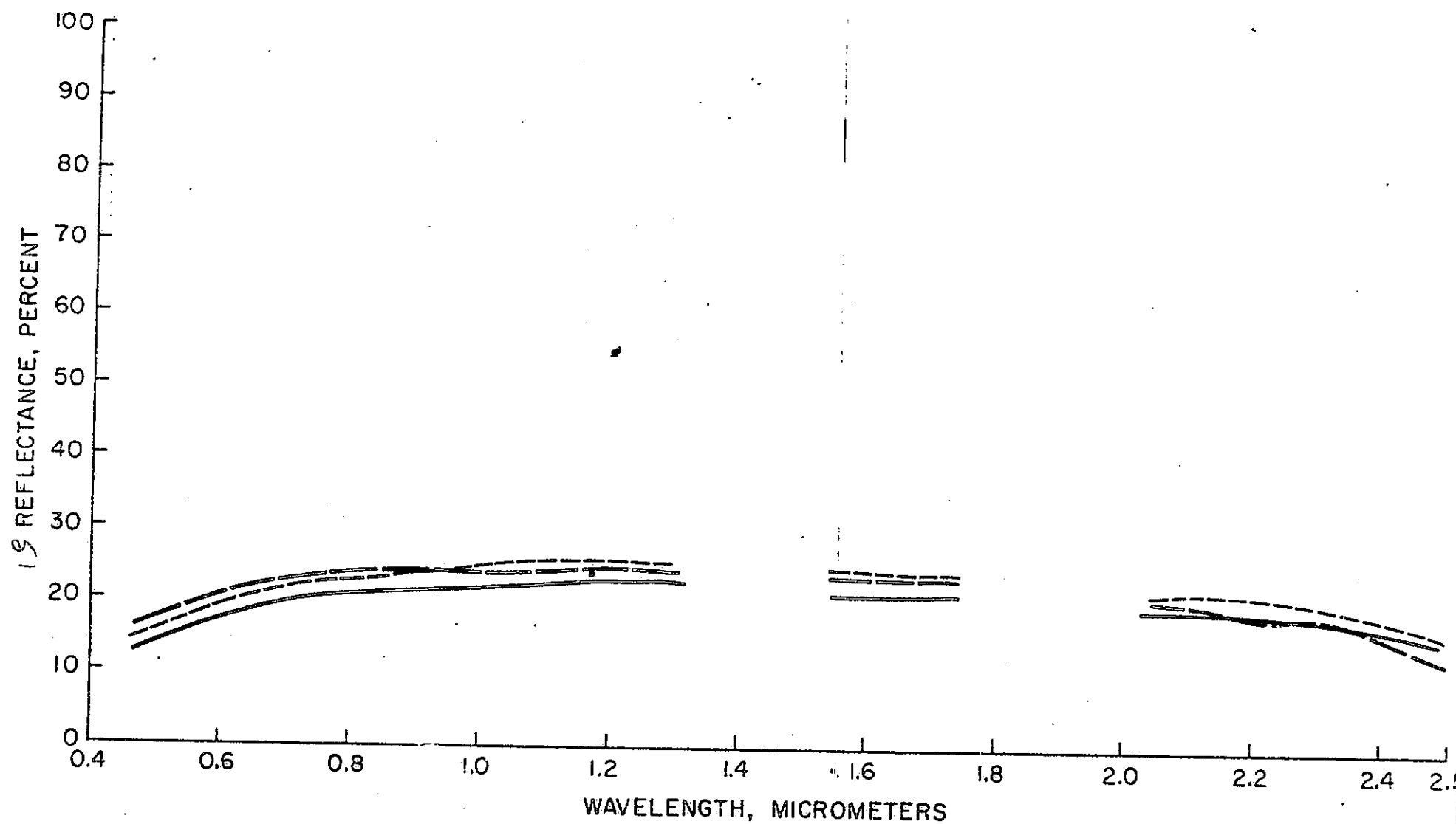


Figure 8 - Representative in situ reflectance spectra for calcitic quartz latite rocks (a) lacking ferric absorption bands (solid line); (b) with a weak 2.2  $\mu\text{m}$  band (long dashed line); and (c) weak ferric absorption bands (short dashed line).

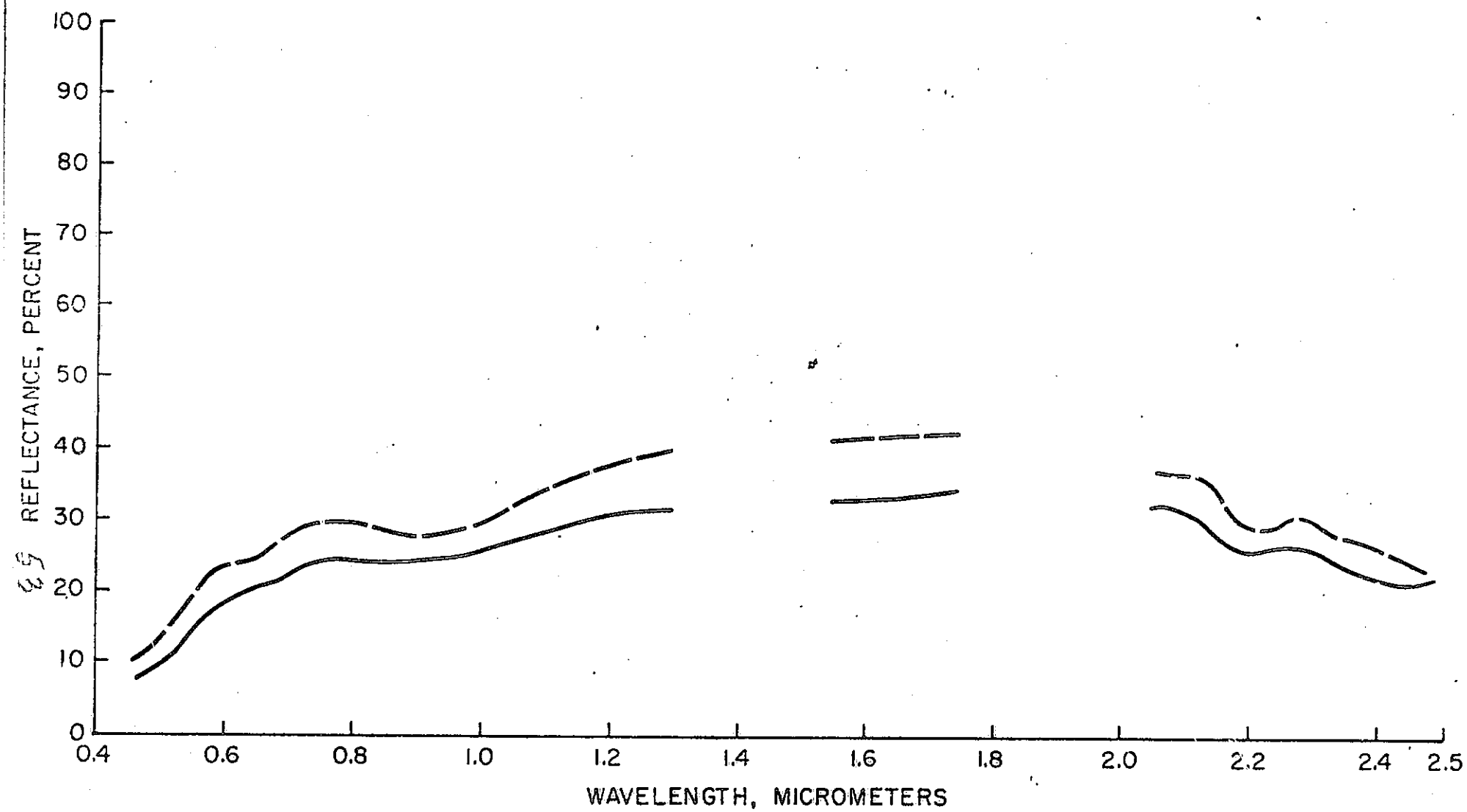


Figure 9 - Representative in situ reflectance spectra for argillized  
latitic tuff in Government Canyon: (a) moderately limonitic (solid  
line) and (b) highly limonitic (long dashed line).

One of the largest areas of argillized rocks forms a crudely elliptical outcrop pattern south of the East Tintic mining district. This area consists mainly of argillized tuff and welded tuff of the Latite Ridge Latite (part of unit Ttm, fig. 3 and table 1). Although several areas of silicified rocks are shown here in the alteration map (fig. 4), the considerable extent of the argillized rocks is not portrayed. Reflectance spectra recorded near the head of Ruby Canyon at the southwest end of the elliptical area (fig. 2) are variable with respect to the intensity of the ferric and hydroxyl absorption bands (fig. 10). In most places, both are well defined (fig. 10a), but locally the ferric bands are less prominent (fig. 10b), or both types of bands are reduced in intensity (fig. 10c). However, judging from field examination and the intensity of the 2.2  $\mu$ m band, this area is more intensely altered than the Government Canyon area.

Argillized rocks along the northeastern extension of the elliptical alteration zone are spectrally similar to those on the southwest end, except that the 2.2  $\mu$ m band is slightly more intense (fig. 11). The pre-alteration rock type was Packard Quartz Latite, rather than units of the Latite Ridge Latite. In general, the plagioclase feldspar and biotite are completely altered to clay minerals and a white bleached mica, respectively, but fresh sanidine and quartz phenocrysts are common.

Big Hill, located about 1.2 km southwest of the North Lily mine in the East Tintic mining district (no. 17, fig. 2), is one of the most conspicuous argillized and locally silicified areas in the study area.

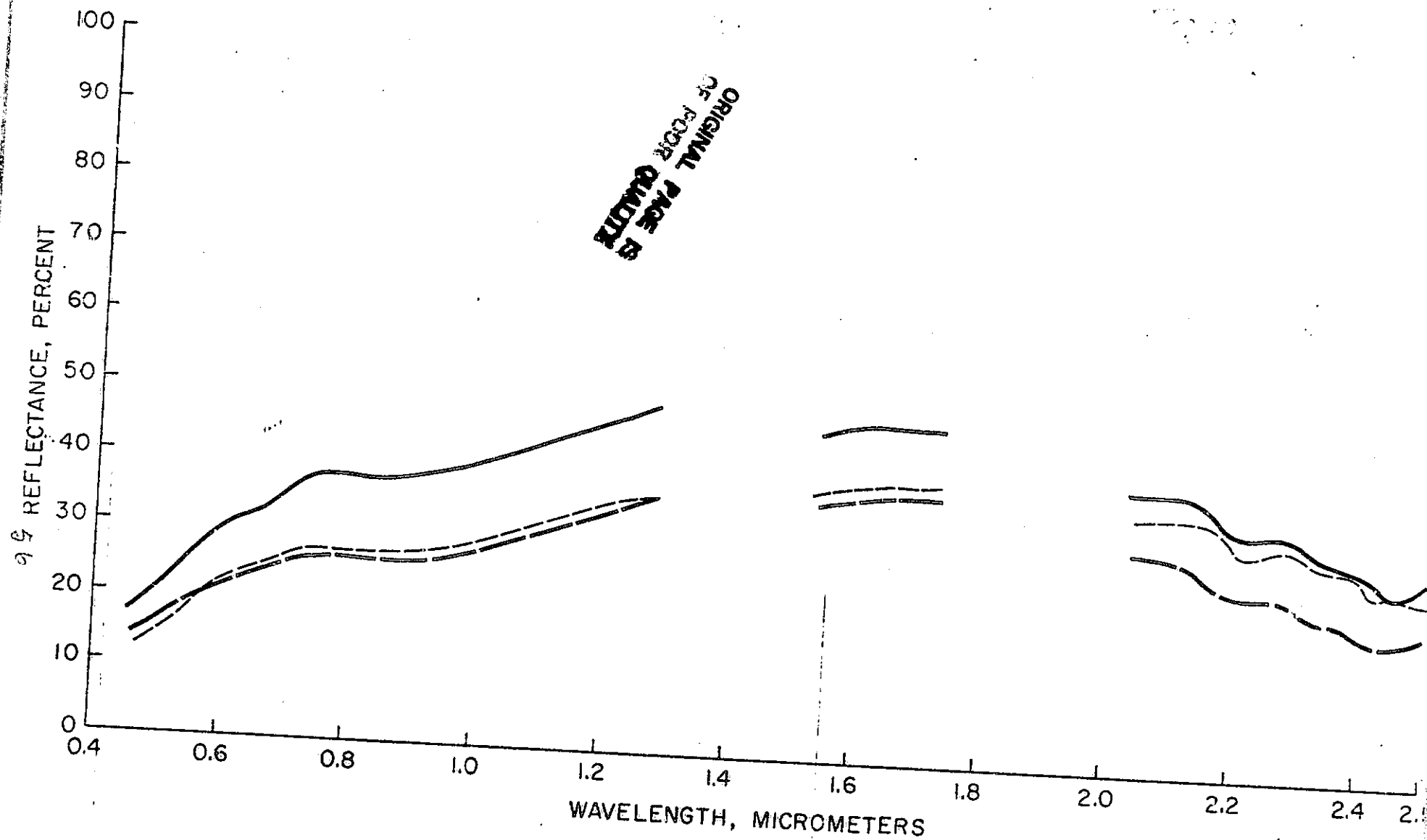


Figure 10 - Representative in situ reflectance spectra for argillized latitic tuff in crudely elliptical area near the head of Ruby Canyon showing (a) intense ferric and hydroxyl absorption bands (solid line), (b) less intense ferric absorption bands (long dashed line), and (c) less intense ferric and hydroxyl absorption bands (short dashed line).

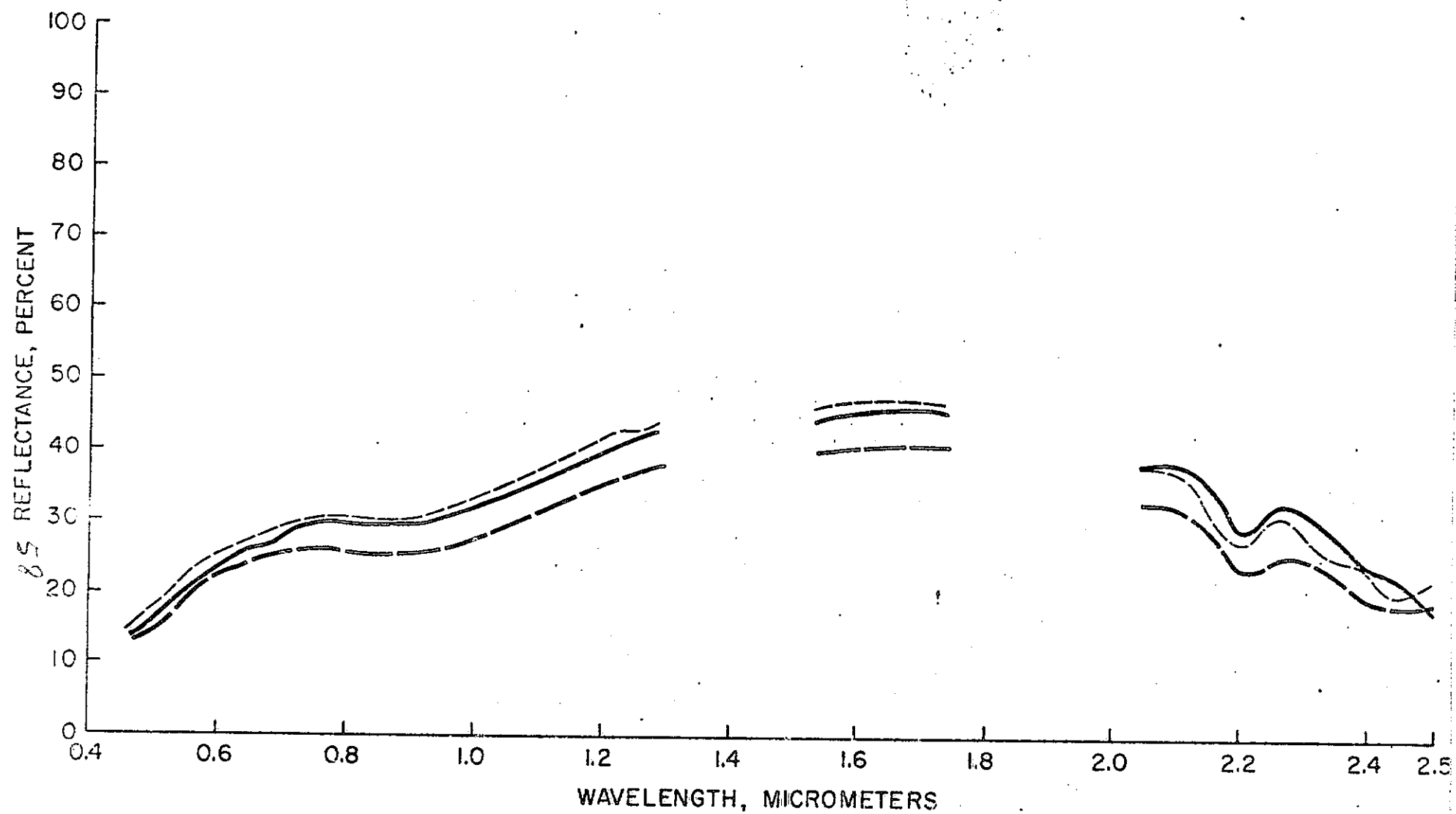


Figure 11 - Representative in situ reflectance spectra for argillized quartz latite at northeast end of crudely elliptical area.

In situ reflectance spectra for the altered Packard Quartz Latite tuffs and flows consistently show broad, intense ferric absorption bands due to the prominence of limonite and jarosite coatings, and a well developed hydroxyl band related to clay minerals, and in places, alunite (fig. 12). Where alunite is present, the hydroxyl band broadens or shifts slightly towards shorter wavelengths (fig. 12c), which is consistent with laboratory spectra for alunite (Hunt and others, 1971) and clay minerals (Hunt and others, 1973). Reflectance at 2.2  $\mu\text{m}$  is commonly 50 percent lower than at 1.6  $\mu\text{m}$ , suggesting a high proportion of hydroxyl phases.

Spectra representing silicified rocks were obtained for only one area located near the North Standard mine (fig. 2). Iron-oxide mineral content is highly variable here, and therefore the intensity of the absorption bands varies from very intense to weak (fig. 13). The hydroxyl band is broad and not as intense as in most of the argillized rocks. Based on the few spectra available for this area, the 2.2  $\mu\text{m}$  reflectance is reduced by 30-40 percent relative to the 1.6  $\mu\text{m}$  reflectance. Various fine-grained silica minerals are dominant in these rocks, but kaolinite and a bleached white micaceous material formed after biotite are present in most places.

Reflectance spectra have not been obtained for many important rock types in the study area. Most important are the iron-oxide stained unaltered rocks, such as the Tintic Quartzite, which are likely to be indistinguishable from the limonitic altered rocks in MSS images. They

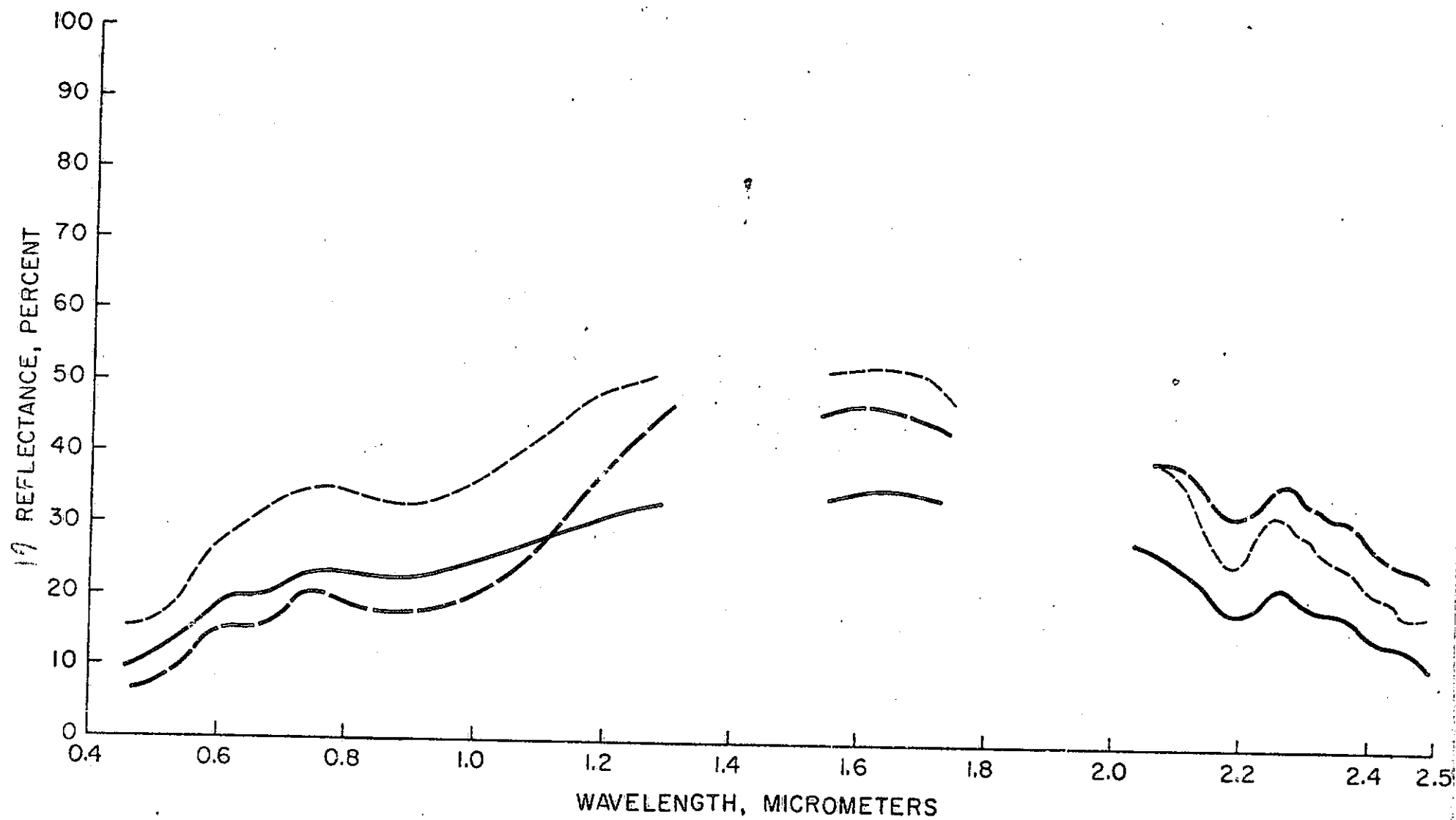


Figure 12 - Representative in situ reflectance spectra for intensely argillized quartz latite tuffs and flows at Big Hill showing (a) moderately intense ferric and hydroxyl absorption bands (solid line); (b) very intense ferric and moderately intense hydroxyl bands (long dashed line); and (c) moderately intense ferric and very intense hydroxyl absorption bands (short dashed line).

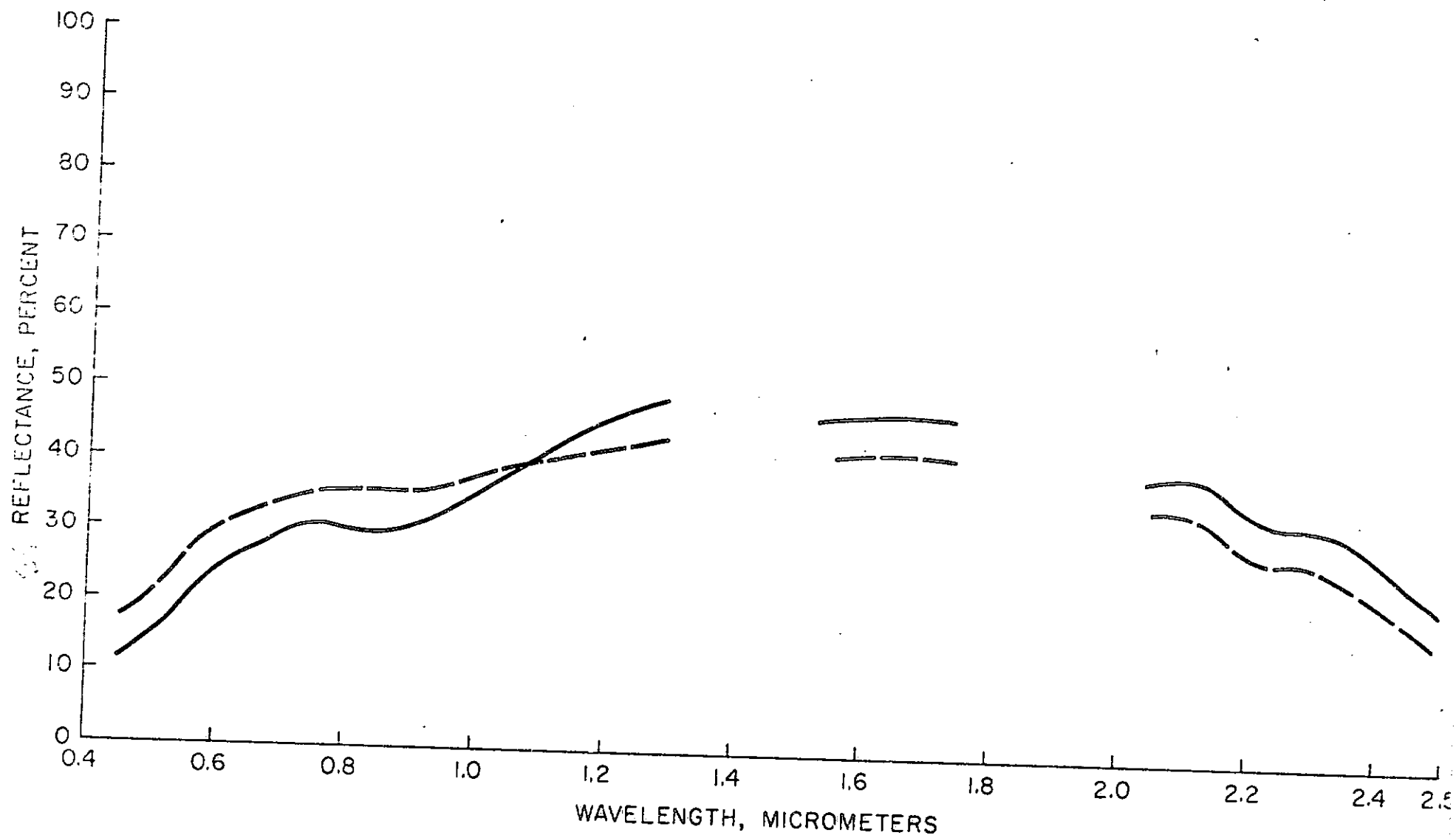


Figure 13 - Representative in situ reflectance spectra for silicified rocks near the North Standard mine showing (a) intense ferric and moderately intense hydroxyl absorption bands (solid line) and (b) weak ferric and moderately intense hydroxyl absorption bands (long dashed line).

might be discriminable, however, in the wavelength region beyond 1.5  $\mu\text{m}$

if the unaltered rocks lack a significant hydroxyl absorption band.

Although a 2.2  $\mu\text{m}$  band is not anticipated in the quartzite, clastic mica present along bedding planes might produce this feature. Also, argillaceous rocks commonly have a weak to moderately intense band in this region owing to the presence of clay minerals (Hunt and Salisbury, 1974; Rowan and others, 1977). Whether or not the magnitude of this spectral feature is comparable in the argillaceous and altered rocks must be determined by additional spectral reflectance measurements. It is noteworthy that the hydroxyl band is commonly masked in medium to dark gray shales by the presence of opaque materials (Hunt and Salisbury, 1974), and therefore might not be present in many of the argillaceous rocks in the study area.

Another possible limitation for using the long wavelength region for discriminating the unaltered and altered rocks stems from the presence of the  $\text{CO}_3^{-2}$  absorption band at 2.35  $\mu\text{m}$  in many carbonate rock spectra (Hunt and Salisbury, 1971). Although this band and the 2.2  $\mu\text{m}$  band are readily distinguishable in reflectance spectra, they are not separable in images that necessarily span both features in order to obtain adequate energy. This situation is further complicated by the presence of the 2.2  $\mu\text{m}$  band, as well as the 2.35  $\mu\text{m}$  band, in argillaceous carbonate rocks.

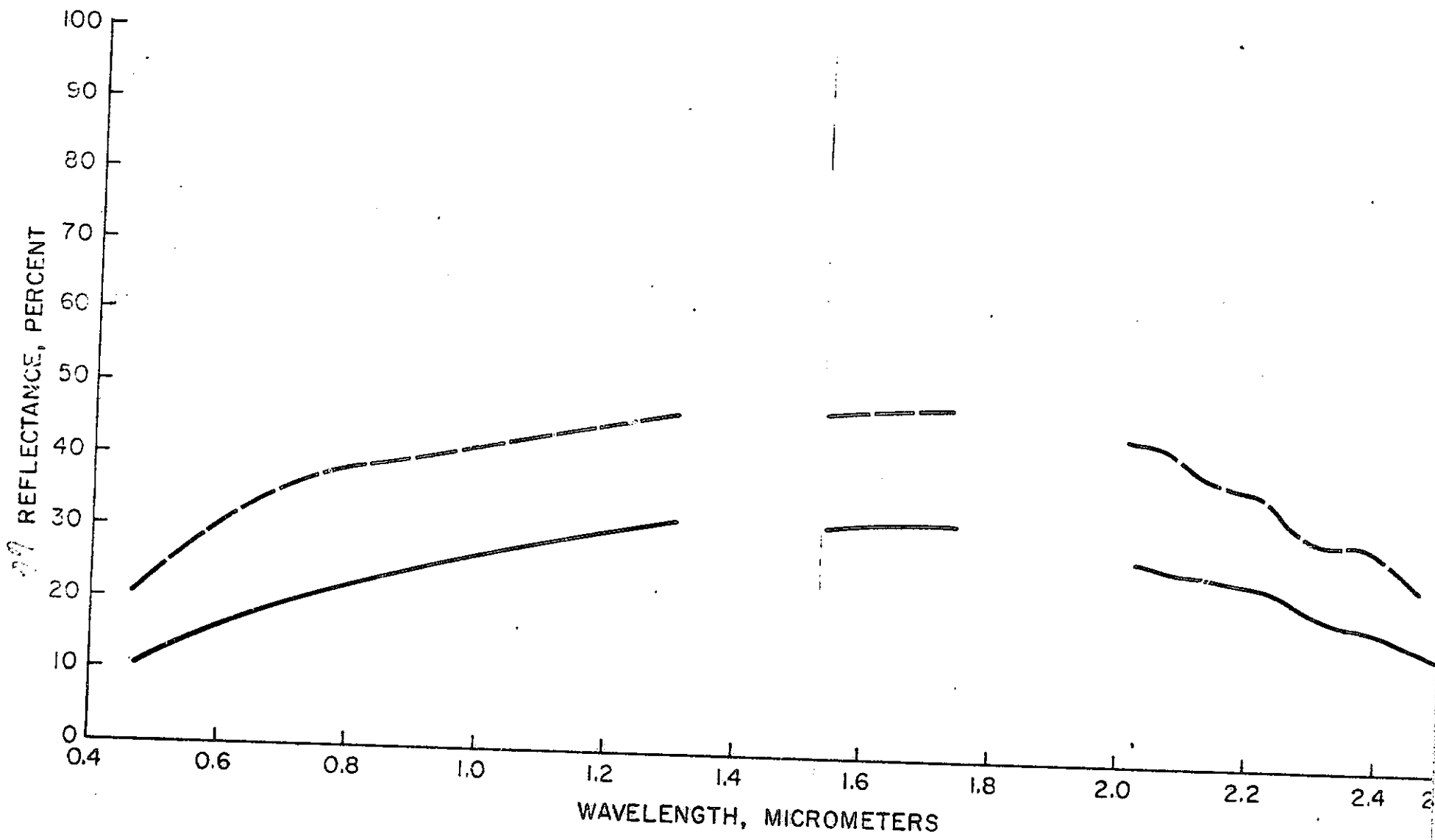


Figure 14 - Representative in situ reflectance spectra for (a) pure limestone (solid line) and (b) limestone fragments and clayey soil (long dashed line).

present (fig. 14a), whereas a weak 2.2  $\mu\text{m}$  band also appears in the spectrum representing limestone fragments and clayey soil (fig. 14b). The overall effect of these bands is depression of the 2.0-2.5  $\mu\text{m}$  reflectance relative to the 1.6  $\mu\text{m}$  level, similar to the decrease described in the altered rocks. These exposures lack anomalous iron-oxide staining, however, and therefore do not have the conspicuous ferric absorption bands typical of most of the altered rocks in the study area.

As in dark shale spectra, the  $\text{CO}_3^{-2}$  absorption band is quenched by the presence of opaque materials. For example, the spectrum representing medium gray, calcite-veined, hydrothermal dolomite lacks prominent absorption bands (fig. 15a) and therefore resembles the unaltered quartz latite spectrum (fig. 6a). On the other hand, light gray hydrothermal dolomite from the same area displays a well-defined 2.35  $\mu\text{m}$  band (fig. 15b). Again, the areal frequency and magnitude of this feature in the study area is not yet known, but is critical to future remote sensing studies.

Only a few in situ vegetation spectra have been obtained in the study area, but judging from spectra obtained in other study areas, these spectra (fig. 16) are generally representative of the main species. Sage, the most common vegetation type, is characterized by low but slightly increasing reflectance in the visible region, the

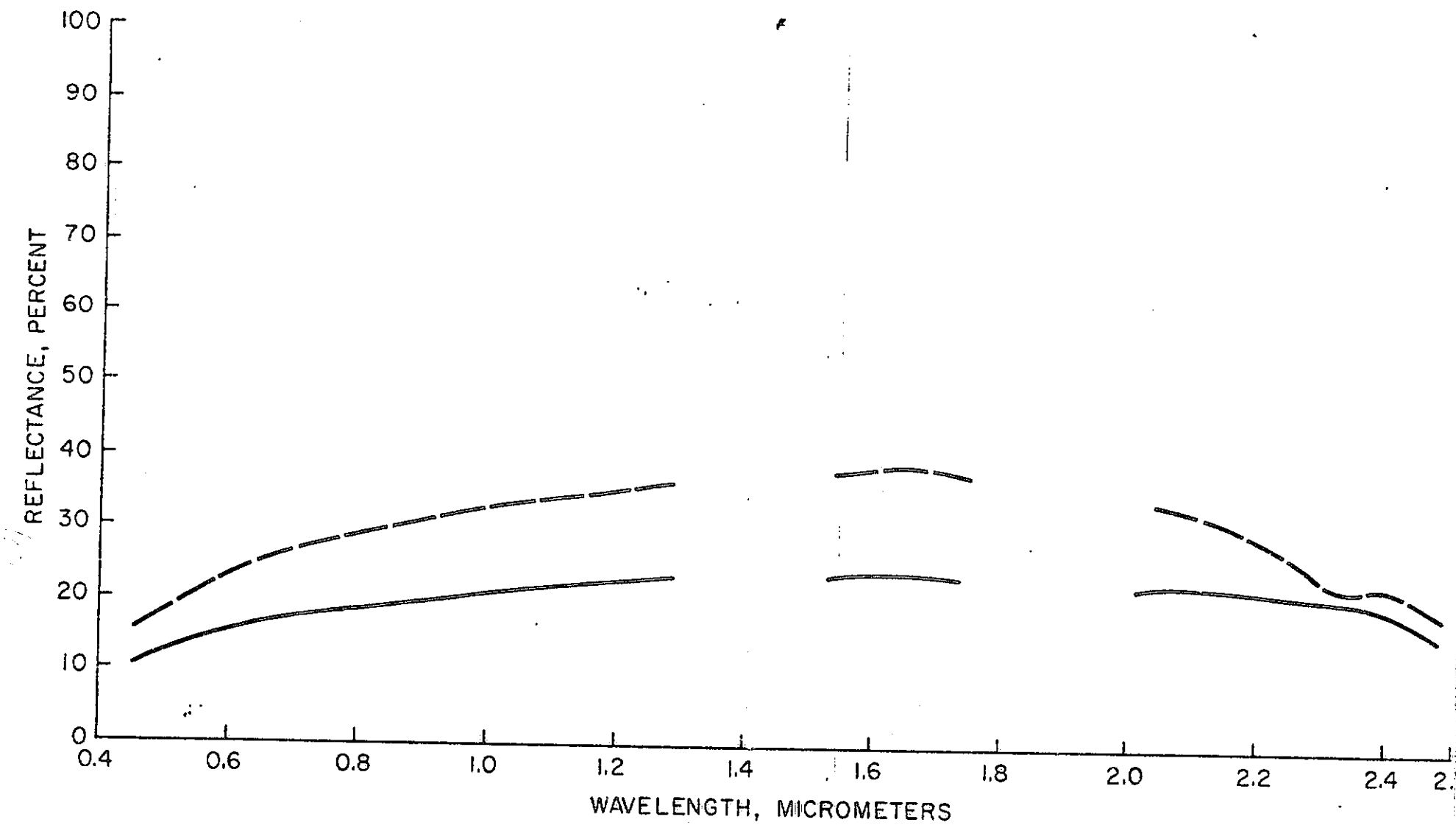


Figure 15 - Representative in situ reflectance spectra for hydrothermal dolomite showing (a) essentially featureless medium gray dolomite spectrum (solid line) and (b) 2.35  $\mu\text{m}$  absorption band in light gray dolomite (long dashed line).

familiar rise between about 0.69  $\mu\text{m}$  and 0.75  $\mu\text{m}$  on the shoulder of the chlorophyll absorption band, slightly increasing reflectance between 0.75  $\mu\text{m}$  and 1.3  $\mu\text{m}$ , and then progressively lower reflectance in the 1.6  $\mu\text{m}$  and 2.2  $\mu\text{m}$  regions (fig. 16a). The decreasing reflectance in the longer wavelength regions and the subtle absorption band near 2.1  $\mu\text{m}$  are due to water in the leaves (Allen and Richardson, 1968).

In general, the shapes of representative juniper and sage spectra are similar, but the spectral features are more pronounced in the juniper spectrum (fig. 16b). There are several differences, however, which provide a basis for differentiating these two vegetation in multispectral images. Most important are the steeper slope between 0.45  $\mu\text{m}$  and 0.55  $\mu\text{m}$ , the decline between 0.55  $\mu\text{m}$  and 0.68  $\mu\text{m}$ , and the large increase in reflectance from 0.68  $\mu\text{m}$  into the near-infrared region in the juniper spectrum. In addition, juniper displays a less steep slope in the 0.85  $\mu\text{m}$  to 1.1  $\mu\text{m}$  region, and a reversal in slope near 1.1  $\mu\text{m}$  due to the presence of water bands near 0.95  $\mu\text{m}$  and 1.2  $\mu\text{m}$  (fig. 16b). The higher water content of juniper also causes very low reflectances in the 1.6  $\mu\text{m}$  and 2.2  $\mu\text{m}$  region.

In summary, ferric iron and hydroxyl absorption bands are prominent in the argillized latite and quartz latite in situ reflectance spectra. However, intense ferric absorption bands are also anticipated in spectra representing iron-oxide stained unaltered

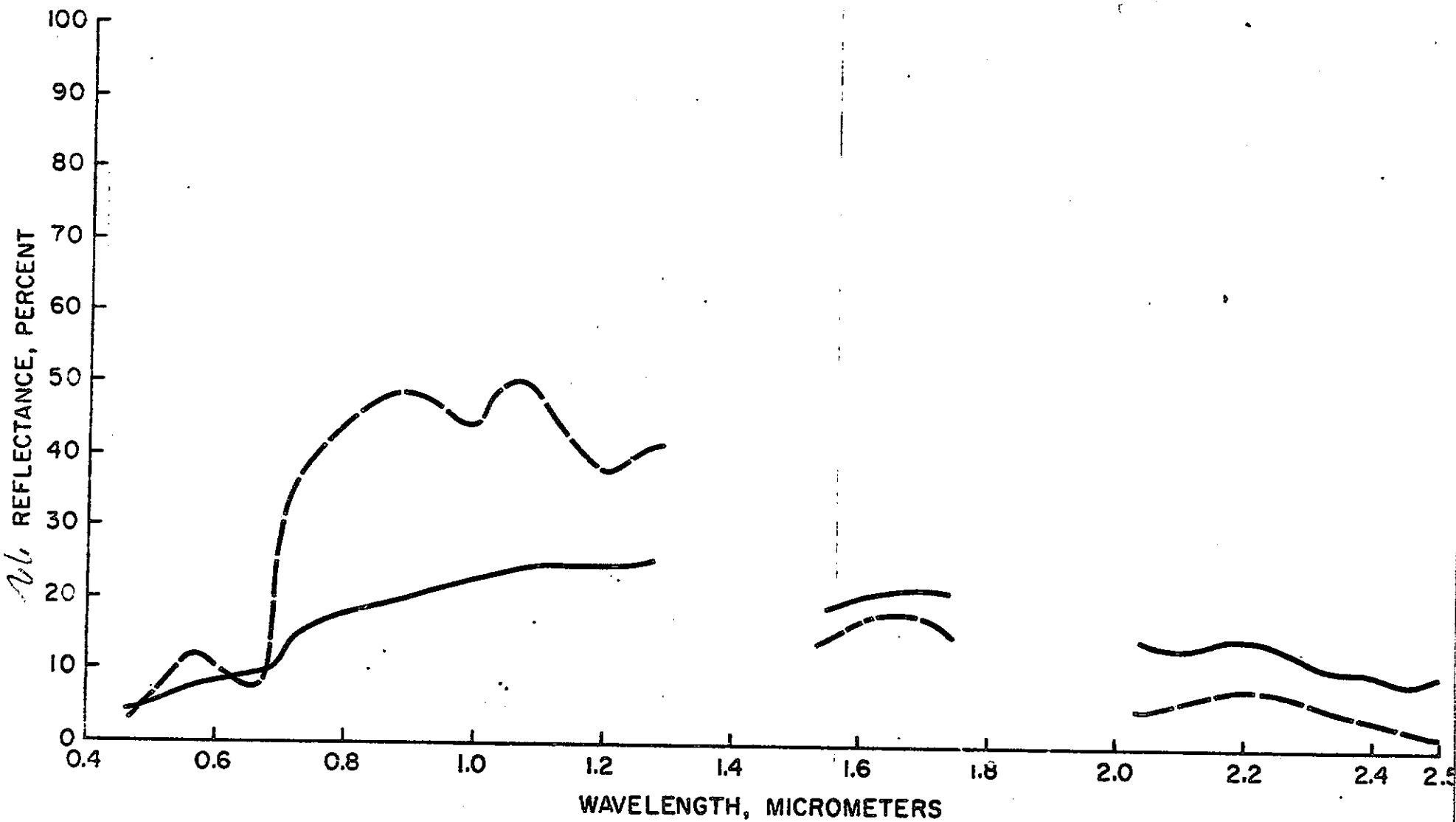


Figure 16 - Representative in situ reflectance spectra for (a) sage  
(solid line) and (b) juniper (long dashed line).

sedimentary and igneous rocks present in the study area. Some of these might be distinguishable from the altered rocks in the 2.0  $\mu\text{m}$  to 2.5  $\mu\text{m}$  region. Others, such as moderate to high albedo shales and carbonate rocks, might not be discriminable in images recorded in this spectral region because of the expected presence of a 2.2  $\mu\text{m}$  feature and a 2.35  $\mu\text{m}$  feature, respectively, in these spectra. In addition, the calcitic volcanic rocks and hydrothermal dolomite appear to lack both the ferric and hydroxyl absorption bands, and therefore are probably not distinguishable from many unaltered rocks in the East Tintic Mountains. Consideration of the limited vegetation spectra presently available for the study area indicate that juniper and pinyon, which is spectrally similar to juniper, pose a more severe problem than sage to detection of limonitic altered rocks in MSS images because inclusion of a few trees in a pixel will significantly change the spectral radiance.

## Image Analysis

In addition to Landsat MSS images, a sequence of color photographs obtained from three greatly different flight altitudes are available for the East Tintic Mountains. Although this section is mainly devoted to evaluation of MSS images, these color photographs deserve comment because of their potential for mapping altered rocks. In addition, the photographs significantly augmented some aspects of the MSS image evaluation.

### Color Photographs

The sources of these color photographs are Skylab, high-altitude aircraft, and low-altitude aircraft. An S190B Skylab color photograph of the study area (fig. 17) shows numerous high albedo areas and pink to red areas that might represent bleached and limonitic rocks, respectively. Many of the high albedo areas correspond to bleached hydrothermally altered exposures, mainly argillized and silicified rocks. Some of the most conspicuous areas are the southern slope below Big Hill (A, fig. 17), which lies within the largest argillized area in the East Tintic mining district (fig. 5), a crudely elliptical area south of Big Hill (B, fig. 17), the argillized latite plug south of Tintic Mountain (C, fig. 17), and a large area in Government Canyon (D, fig. 17). The Big Hill and latite plus areas were well documented through previous field mapping (fig. 4), but only a small part of the

elliptical area was previously mapped, and no alteration was shown in Government Canyon (fig. 4). Field examination shows that both of these areas consist of bleached pyritic altered rock.

On the other hand, large areas underlain by high albedo sedimentary rocks are indistinguishable from the bleached altered areas. For example, note the exposures of sedimentary rocks south and west of Pinyon Peak (E and F, respectively, fig. 17). This problem is accentuated by illumination variations due to topographic slope. Note, for example, that the crest and eastward-facing slope of Quartzite Ridge and the ridges to the north are very bright, whereas the opposite slopes are dark.

Another important limitation of the Skylab photograph is that most of the altered areas are substantially more extensive than the high albedo areas. More importantly, some of the altered rocks have only moderate albedo, and therefore are not distinctive in the photograph. Two examples are the pyritized breccia pipe southwest of Tintic Mountain, and silicified rocks southeast of Pinyon Peak (G and H, respectively, fig. 17).

In spite of its high spatial resolution, very little color information is provided by the S190B color photograph, mainly because of atmospheric attenuation, low sensitivity in westward-sloping areas, and saturation where high albedo materials slope sunward. Three general color categories can be discerned: (1) dark blue-green vegetated areas, (2) white sunward slopes, and (3) pink to red areas.

*See Attached Color Plate*

Figure 17 - Skylab S190B color photograph of the study area showing high albedo argillized areas. A, Big Hill; B, elliptical area; C, latite plug; D, Government Canyon, high albedo sedimentary rocks; E, south of Pinyon Peak; F, west of Pinyon Peak, and low to moderate albedo altered areas; G, pyritized breccia pipe; and H, silicified area southeast of Pinyon Peak.

The pink to red variation depends more on topographic slope variations than on the degree of iron-oxide staining present, and hence is not a reliable basis for mapping limonitic rocks. For example, no color difference is apparent in the photograph between the sedimentary rocks west of Pinyon Peak (F, fig. 17) and most of the exposures in the Big Hill and elliptical altered areas (A and B, respectively, fig. 17), even though the rocks and soils have markedly different colors.

Color-infrared photographs were acquired by the S190A camera, but because of their lower spatial resolution, they are less useful than the S190B color photographs for mapping altered rocks. The color-infrared photographs are useful, however, for detecting areas of vigorous vegetation.

High-altitude color (fig. 18) and color-infrared photographs acquired during the spring and fall have proven very useful for location purposes, and the latter photographs for mapping vegetation, but low contrast and poor color fidelity severely limit their value for distinguishing other surface materials. High-altitude color photographs of the Battle Mountain-Eureka, Nevada mineral belt are of similar poor quality. In contrast, photographs obtained of the south-central Nevada and Virginia Range, Nevada study areas are of good to excellent quality. This variation in quality of high-altitude color (and color-infrared) photographs is common, and emphasizes the difficulty of determining optimum film-filter combinations, exposures, processing, etc. for widely different terrain, atmospheric, and solar illumination conditions.

ORIGINAL PAGE IS  
OF POOR QUALITY

See Attached Color Plate



Figure 18 - High-altitude color photograph of the study area.

Low-altitude color photographs have been widely used in exploration mapping because textural as well as color differences are usually well displayed; however, color photographs obtained simultaneously with 24-channel multispectral scanner images of the study area display only the most conspicuous colors. One of these photographs is shown in a later section (fig. 28), in conjunction with evaluation of the CRC image of the East Tintic mining district.

### MSS Images

The general procedure followed in computer processing and evaluation of MSS images of the study area is outlined below:

1. Band-to-band comparison of EROS Data Center black-and-white images;
2. Digital density slicing of MSS band 5 image for albedo information;
3. Evaluation of a linearly stretched color-infrared composite image;
4. Color-compositing of stretched ratio images using diazo films;
5. Extraction of green pixels from the optimum color-ratio composite (CRC) image to show the areal distribution of limonitic rocks; and
6. Comparison of the resulting map with the alteration maps shown in figures 4 and 5.

In most respects, this procedure is similar to that used in south-central Nevada (Rowan and others, 1974). However, several specific changes are noteworthy because they were prompted by the geological and environmental conditions in the East Tintic Mountains, and by the need for improved mapping precisions. The two most important modifications are the use of large format, high geometric precision

images, and a different combination of stretched black-and-white ratio images in the optimum CRC image than was used in the south-central Nevada study.

Individual MSS Band Images - Band-to-band comparisons of the standard image products for the study area yield results similar to those reported for south-central Nevada (Rowan and others, 1974): no spectral radiance differences are apparent among rock units because the differences that are shown in the field spectra (fig. 6-15) are subdued by the broad MSS bandpasses, and by integration of spectrally different materials in individual pixels. The only spectral contrast seen in these images is the low radiance of vegetation in the visible wavelength bands (MSS 4 and 5) relative to high radiance in the near-infrared bands (MSS 6 and 7). Although contrast stretching increases the spatial detail, no significant enhancement of spectral radiance variations resulted.

As indicated by analysis of the color photographs, variations in the overall brightness level or albedo has proven to be of limited value for mapping altered rocks because both altered and unaltered rocks span broad albedo ranges; however, the digital format of MSS data allows a more precise evaluation. In sparsely vegetated areas, MSS band 7 images typically have higher albedo

contrast than the other three bands. However, because of the high near-infrared reflectance of vegetation, MSS band 5 images are better suited for studying albedo variations in more densely vegetated areas.

Figure 19 shows an MSS band 5 image of the study area which has been linearly contrast-stretched to enhance albedo differences and spatial detail. This image, shown here at 1:100,000 scale, was originally recorded at approximately 1:158,000 scale on 53x53 cm positive film, with minimum and maximum densities of 0.30 and 1.42, respectively. The plotter used, a Geospace GS-34/10, has a precision of  $\pm 0.127$  mm measured along the diagonal, which, in the 48 pixel/25.4 mm playback mode, is equivalent to about  $\pm 0.25$  of a pixel.

The large format and high geometric precision greatly facilitate photographic reproduction of color composites. Consequently, CRC images generated from black-and-white ratio images can be used at either small scales for reconnaissance studies, or at large scales for detailed evaluations.

A convenient method for evaluating albedo variations recorded by the MSS combines digital density slicing for displaying radiances above a specific level, and contrast stretching of all lower values for retaining topographic detail. In figure 20, the threshold value,



ORIGINAL PAGE IS  
OF POOR QUALITY

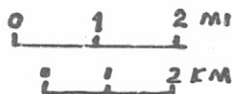


Figure 19 - Linearly stretched MSS band 5 image of the study area.

digital number (DN) 88, was selected because it appears to represent a moderately high albedo altered area (A, fig. 20). Thus, areas having higher DNs are displayed as dark pixels, and lower values are represented by lower film densities. A linear stretch was applied to all values below DN 88.

Comparison of the density sliced image (fig. 20) and alteration map (fig. 4) shows that most of the altered areas in the East Tintic Mountains have MSS band 5 radiances greater than DN 88. As previously noted, several high albedo altered areas are not shown in the alteration map (B, fig. 20), although this difference is mainly due to exclusion of most argillized areas in the field compilation. On the other hand, many of the black pixels represent unaltered rocks. Most of these areas are east to southeast-facing slopes, such as those south of Pinyon Peak and along the east front of Tintic Mountain (C and D, respectively, fig. 20). Other areas consist of intrinsically high albedo unaltered materials, such as limestone and shale.

From the exploration point of view, it is perhaps more important that some of the altered areas have radiances less than the threshold level and therefore are not distinguished in the density-sliced image. For example, note that the vein deposits east of the control area and south of Ruby Canyon are not shown (E and F, respectively, fig. 20), and the silicified zones north of Ruby Canyon are only partially displayed (G, fig. 20). Although lowering the threshold value would



ORIGINAL PAGE IS  
OF POOR QUALITY

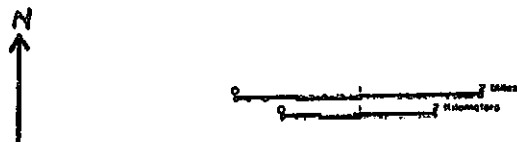


Figure 20 - MSS band 5 image for part of the study area with pixels greater than DN87 shown in black and pixels of lower values linearly stretched over the remainder of the film density range. A, locates threshold pixel with DN88; B, altered areas with DN values  $\geq 88$  shown in figure 18; C, sedimentary rocks on south-facing slopes; D, volcanic rocks on south-facing slopes; E and F, vein deposits; G, silicified deposits.

alleviate this problem, a much greater number of pixels representing unaltered rocks would then be above the threshold. Therefore, in the East Tintic Mountains, the usefulness of MSS band 5 albedo for mapping altered areas is limited by the fact that some altered areas would be missed, and many areas of unaltered rocks would be misrepresented as being altered, mainly because of slope effects and overlapping albedo ranges. Results of similar studies in the Virginia Range, Nevada, are more positive, whereas those in the Battle Mountain-Eureka, Nevada, mineral belt are distinctly negative. Thus, the value of albedo mapping for distinguishing altered and unaltered rocks depends greatly on the area under study, but is hampered by even moderate topographic relief. In addition, this approach provides little or no mineralogical information.

Color-infrared composite MSS images have more potential than individual black-and-white MSS images for mapping altered rocks because the spectral information of three bands are displayed simultaneously in color, rather than singly as levels of gray. However, superposition of large radiance variations due to topographic slope and albedo on the spectral differences obscures all but the most marked spectral contrast. Consequently, vigorous vegetation and vividly colored limonitic rocks and soils are apparent in color-infrared composite images by their respective red color and yellow to orangish-yellow color; less marked spectral contrast is not apparent, however.

In the East Tintic Mountains, the altered rocks are characterized more by bleaching and subdued ochreous colors rather than by the vivid red, orange, and yellow colors seen in some hydrothermally altered areas. Therefore, the altered areas lack distinctive colors in the contrast-stretched color-infrared composite image shown in figure 21.

See Attached Color Plate

ORIGINAL PAGE IS  
OF POOR QUALITY

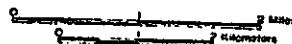


Figure 21 - Color-infrared composite image of the study area made in a color-additive viewer using MSS bands 4, 5, and 7 in blue, green, and red, respectively.

Color-Ratio Composite Images - Development of the color-ratio composite technique was stimulated by the need for subduing brightness variations due to topographic slope and albedo, while enhancing small spectral reflectance differences among rocks, especially those of limonitic rocks (Rowan and others, 1974; 1977). Initially, 70 mm black-and-white stretched-ratio images were used to produce diazo color films, registered at high magnification, and photographically enlarged to a suitable working format, usually 50 cm (approximately 1:500,000 scale). Although CRC images made using this procedure have proven very useful for detecting limonitic altered rocks at small reconnaissance scales, their value for detailed studies is limited by several factors relating to the large magnification used.

Three general categories of problems result from the earlier procedure: (1) internal misregistration of the composite, which results in incorrect color coding of pixels; (2) poor color fidelity due to vignetting in the copy-camera lens; and (3) geometric distortion of the enlargements caused by camera lens distortion. In spite of careful registration using a microscope, slight misregistrations amounting to several pixels arise from imprecision of the film playback instrument and differential stretching and contraction of the ratio image films, diazo films, and bonding material, usually cellophane tape. This degree of misregistration means that, although large areas may be correctly colored, many individual pixels will be incorrectly coded; therefore, some small, but important limonitic areas would be missed, and some non-limonitic areas would be misrepresented.

Although loss of color fidelity through enlargement is not as critical as misregistration, it hampers interpretation, especially around the outer parts of the enlargement where colors commonly become darker and less distinct. Geometric distortion of the enlargement is important because it bears directly on the ability to transfer the CRC information to base maps.

The previously described large format image playback capability provides a means for overcoming most of these problems. For the East Tintic Mountains study area, two CRC images, each covering approximately one-fourth of a Landsat scene, were made using 20x25 cm sheets of diazo film. Registration was ensured by pin-punching the original ratio images to each other and the diazo films to the respective images. The film was held in contact with the ratio image in a vacuum frame and exposed to an integrating ultraviolet light source. Developing of the exposed diazo film was achieved using a conventional ozalid machine. Internal registration of the 20x25 cm CRC images is estimated to be within one-fourth of a pixel (approximately 0.13 mm).

The first CRC image of the study area consisted of blue, yellow, and magenta diazo films representing linearly stretched MSS 4/5, 5/6, and 6/7 ratio images, the same combination used for the south-central Nevada scene (Rowan and others, 1974, 1977); however, most limonitic rocks appeared blue, like many of the unaltered rocks, rather than green, as anticipated from the south-central Nevada results. A second composite, in which MSS 4/6 was substituted for MSS 5/6, displays the

limonitic rocks as distinct green pixels, although more alluvium also appeared green than in the initial CRC image. Similar results have been reported by Ashley and others (1977, written comm.) for the same combinations in the Virginia Range, Nevada. Krohn and others (1977, written comm.) described moderate success using the MSS 5/6 combination in the Battle Mountain-Eureka, Nevada mineral belt, but the green pixels were much less distinct than in the CRC that included the MSS 4/6 ratio image. Yet, the MSS 4/5, 5/6, and 6/7 combination has been used very successfully in sparsely vegetated arid areas in northern Sonora, Mexico (Raines, in press), Saudi Arabia (Blodgett and others, 1975), and Iran (Pohn, 1977, written comm.).

This discrepancy appears to be related to differences in vegetation cover and the method used to determine the contrast stretch parameters. Contrast stretching is performed on the ratio values to increase the contrast of a selected part of the frequency distribution. In the commonly used type of stretch, referred to as an automatic linear stretch, a certain percentage of the highest and lowest values are assigned to black-and-white to permit expansion of the intervening values (Goetz and others, 1975). The percentage of saturated data is usually 2-10 percent of the total number of data points. The expansion or stretch is usually linear, although any of several other functions may be used, depending on the position of the ratios of interest in the distribution.

Automatic linear stretches of ratio values for sparsely vegetated areas usually result in the desired enhancement of limonitic areas because the distributions are approximately Gaussian, and ratio values

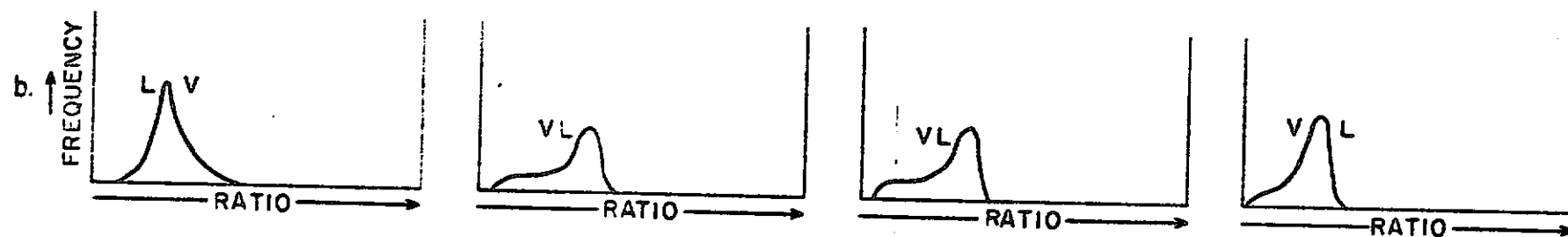
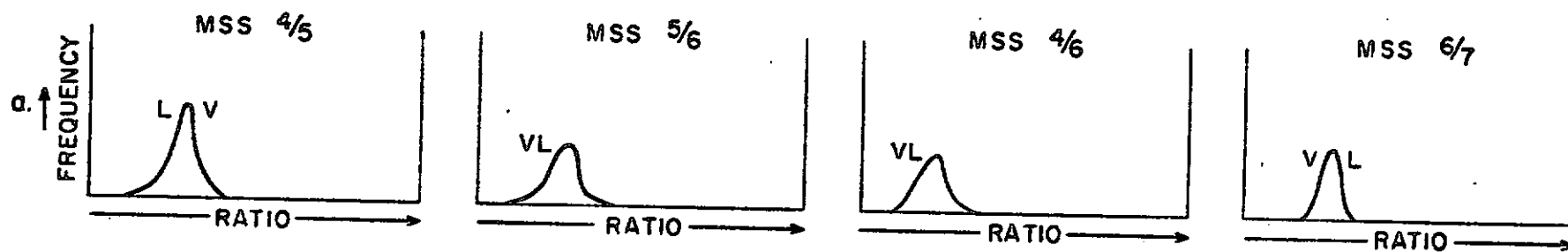


Figure 22 - Schematic frequency distributions for MSS ratios 4/5, 5/6, 6/7, and 4/6 representing (a) areas with sparse vegetation and (b) moderately vegetated areas. V and L locate vegetation and limonite, respectively.

representing limonitic rocks are favorably positioned in the distribution. For example, in MSS 4/5 ratio distributions, limonite typically has the lowest values (fig. 22), and consequently appears very dark in the automatically stretched images. MSS 5/6 limonite values are also low. Conversely, in MSS 6/7 ratio distributions, limonite values are typically high, and therefore result in bright areas in these images.

As vegetation becomes more abundant, the distributions become bimodal or skewed, and in MSS 5/6, vegetation rather than limonite is represented by the lowest values (fig. 22b). Application of an automatic linear stretch to a distribution such as this results in saturation of vegetation pixels in the MSS 5/6 image, but limonite pixels remain just below the medium gray level; thus, there is little or no enhancement of the limonite pixels. Because of the large amount of vegetation in the scene including the East Tintic Mountains, the initial MSS 5/6 ratio image, in which a 3 percent automatic linear stretch was used, contains little information about the locations of limonitic rocks, since these pixels were near medium gray. More enhancement of these pixels was achieved by applying a very severe stretch (table 3) of the low 5/6 ratio values that saturated nearly all of the pixels representing vegetation and increased the density level of those representing limonitic rocks. However, this ratio image was very noisy owing to the generally low spectral radiance contrast of rocks between MSS bands 5 and 6.

A similar evaluation of the MSS 4/6 ratio distribution showed that, although vegetation occupies the lowest part, limonite was, as expected from the reflectance spectra (figs. 9-12), in a slightly lower value range than in the MSS 5/6 distribution. When a 3 percent automatic linear stretch was applied, the limonitic areas appear moderately dark in the MSS 4/3 image, but use of the harsh stretch indicated in table 3 provided even greater enhancement. Although this stretch was as severe as in the MSS 5/6 image, less degradation of the image quality resulted because of the higher MSS band 4 to 6 contrast. Thus, the optimum CRC image for the East Tintic Mountains consists of MSS 4/5, MSS 4/6, and MSS 6/7, displayed as blue, yellow, and magenta diazo films (fig. 23).

Another important procedural modification is use of a color scanner for extracting the colors of interest from CRC images, thereby reducing the subjectivity of visual extraction techniques used in the past. The color scanner being used is the Linoscan 204, available at the E.I. DuPont de Nemours and Company Graphics Center, Bethel, Pennsylvania, that records selected colors or color ranges from either transparencies or prints onto high contrast black-and-white film. Two resolution settings, approximately 20 and 40 lines per millimeter, provide the capability for readily displaying individual pixels. The largest acceptable image is 31 cm by 46 cm, and the scan speed is 23.6 sec per centimeter. Up to four black-and-white images representing

Table 3

Parameters for linear stretches used for  
black-and-white MSS images of the study area

MSS Ratio	Stretch Limits Ratios x 100	Gain - Offset		% Saturation	
				0 DN	255 DN
4/5	73-113	635.7	465.0	0.6	18.7
5/6	75-123	531.2	398.4	25.6	1.0
4/6	76-108	796.8	605.0	26.7	1.6
6/7	97-127	850.0	824.0	22.6	2.0

different colors can be played back simultaneously by limiting their format to about 15 cm by 15 cm; larger formats limit the number of playback images.

In order to extract the green pixels from the optimum CRC image (fig. 23) representing limonitic rocks, a contact Cibachrome print was scanned, as misregistration resulted when the original diazo composite was wrapped around the scanner drum. The resulting black-and-white image, essentially a limonitic materials map, shows pixels ranging from light to dark green in alluvial, as well as outcrop areas, at the 158,000 scale of the CRC image (fig. 24). Pixels occurring in alluvial areas were subsequently deleted using high altitude photographs, and the resulting limonitic bedrock map (fig. 25) was enlarged to 1:100,000 scale to facilitate comparison with the alteration map (fig. 4).

Raines (1977, written comm.) has developed another method for extracting variously colored pixels by computing the Munsell color-space formula for the pixels of interest. Although this approach has the advantage of being more useful for relating the digital values of given colors, it is substantially more expensive. Both techniques provide internally consistent, repeatable results, an illusive objective using visual techniques, but, in both cases, selection of representative pixels is accomplished visually.

see Attached Color Plate

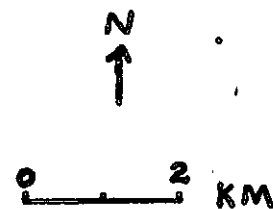
ORIGINAL PAGE 13  
RE. EOE 1000 1000 1000

Figure 23 - Color-ratio composite image of the study area made using blue, yellow, and magenta diazo colors for MSS ratio images 4/5, 4/6, and 6/7, respectively. ID E-1735-17335. Recorded 28 July 74.



Figure 24 - Map of the study area showing the distribution of green pixels in the color-ratio composite image (fig. 23). Green pixels extracted using the Linoscan scanner. Approximate scale 1:158,000.

ORIGINAL PAGE IS  
OF GOOD QUALITY



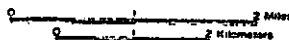


Figure 25 - Map of the study area showing the distribution of pixels representing limonitic bedrock and associated residual soil. Green pixels representing alluvial deposits deleted from figure 24. Approximate scale 1:100,000.

Evaluation of Limonitic Bedrock Map - Comparison of the limonitic bedrock map (fig. 25) with the alteration map (fig. 4) shows that most of the silicified areas were detected, at least in part. In some places, such as on both sides of the railroad southeast of Pinyon Peak, the agreement between the distribution of pixels representing limonitic rocks and the mapped silicified zones is striking (A, fig. 26).

The most important differences between the two maps are that (1) some altered areas are not depicted in the limonitic bedrock map, and (2) numerous pixels representing limonitic rocks are not coincident with altered rocks mapped in the field. The first discrepancy is almost entirely attributable to obscuration of the altered rocks by vegetation cover, although in some places, small exposure size and lesser amounts of limonite stain are contributing factors. It is important that, because of the distinctive spectral reflectance of limonite, drab-colored limonitic, as well as vividly colored surfaces, are readily detected in the CRC image.

In order to estimate the amount of vegetation cover that obscures the limonitic bedrock in the CRC image (fig. 26), areal density counts were made in critical areas using ground traverses and hand-held aerial photographs in areas mainly populated by shrubs, and aerial photographs where pine trees are dominant. The procedure followed in the shrub areas consisted of categorizing materials as to viable vegetation, dead vegetation debris, or rock and soil at 1.0 m intervals along

*See attached Color Plate*

Figure 26 - Map of the study area comparing the distributions of altered areas and veins mapped in the field (shown in fig. 4) with pixels representing limonitic rocks (shown in fig. 25). Gray represents altered areas mapped in the field; magenta represents limonitic rocks. A, silicified rocks southeast of Pinyon Peak; B, silicified rocks obscured by vegetation; C, small areas of silicified rocks; D, area of mixed unaltered volcanic and altered volcanic rocks; E, well-exposed vein deposits; F, argillized rocks in crudely elliptical area; G, argillized latitic tuffs; H, argillized quartz latite; I, argillized latite plug; J, limonitic weakly altered quartz latite; K, limonitic quartz latite; L, Dragon mine; M, Iron King #1 mine; N, hydrothermal dolomite; O, north-trending Tintic Quartzite; P, pink quartz latite flow rock.

25 m traverses. The procedure was then repeated along the same traverse at 1.0 m spacings, offset from the initial marks by 0.5 m. Finally, the percentage of each category was calculated and used to characterize the sample area. Ten areas, totaling 2625 counts along traverses, were sampled in this manner.

The ground measurements were supplemented in a few areas by density slicing color-infrared transparencies acquired from a light aircraft using a hand-held 35 mm camera. The spatial resolution of these photographs is adequate to separate soil and rock from vegetation, but vegetation could not be subdivided into viable and debris categories.

The results of the ground measurements indicate that total shrub cover, both viable and debris, greater than approximately 45 percent, obscures limonitic altered rocks in the CRC image (fig. 23). Percentages determined by density slicing of the hand-held photographs were within 1-2 percent of this value. This estimate is consistent with the results of Siegal and Goetz (1977), based on evaluation of ratios calculated from field spectra for varying amounts of vegetation cover on limonitic argillized rocks.

Some large silicified areas are obscured by substantial stands of pinyon and juniper trees, plus sparse shrub undergrowth. The largest such region is located south of Ruby Hollow east of Treasure Hill (B, fig. 26). Although three pixels representing limonitic debris in clearings are shown in the limonitic bedrock map, silicified areas as large as 300 m are obscured by trees and shrubs. The areal densities

of trees and shrubs are estimated to be 28 and 10 percent, respectively, yielding a total cover of approximately 38 percent. Thus, the limiting values for this and similar areas is approximately 38 percent. The slightly lower limiting value in the pinyon and juniper area may be due to the larger departure of their MSS 4/5, 5/6, and 6/7 ratios from typical limonitic ratios than would be expected for shrub cover dominated by sage (fig. 16a and b).

Judging from repetitive counts along several traverses in shrub areas, the margin of error appears to be on the order of +5 percent. Although the accuracy of the determination for the pinyon and juniper area has not been tested, a similar degree of variation is anticipated. Thus, the above values should be stated as 40-50 percent and 33-43 percent for shrubs and pinyon and juniper populated areas, respectively. The amount of vegetation cover that can be tolerated using the MSS data also depends on the amount and type of limonite stain in the altered area. Obviously, small amounts of limonite stain will be obscured by more modest vegetation cover and, conversely, highly limonitic areas will be detectable with more substantial cover; however, the relationship between amounts of limonite and vegetation cover has not yet been determined for the MSS bandpasses.

Numerous mapped silicified areas are not portrayed in the limonite map because they are smaller than the nominal MSS spatial resolution. However, several areas larger in horizontal extent than the nominal

resolution were not detected in areas with slightly less apparent vegetation cover than is present in the vegetation sample areas. Evidently, the position of the individual pixels in these undetected altered areas is such that the proportion of limonitic altered rocks is small relative to the amount of vegetation, in spite of the overall slightly less dense cover. This situation is exemplified by the northeast-trending zone of small silicified areas between Fremont and Rattlesnake Canyon (C, fig. 26). Only the largest, most closely spaced altered areas near the northeast and southwest termini were detected. In some areas along this mainly sedimentary rock zone, the problem is compounded by the presence of lesser amounts of limonite than is typical of the altered volcanic rocks.

Another factor that makes detection of some limonitic silicified zones difficult is mixing of unaltered colluvium with the altered rocks. For example, most of the large silicified area southeast of Pinyon Peak that was detected by only a few pixels in the CRC image (D, fig. 26) consists of light yellowish-brown to medium brown rock fragments, mainly less than 15 cm across, light brown to light yellowish-brown soil, and roughly 25 percent shrub cover. Outcrops are sparse, and only about 100-200 m in their largest dimension. Mixed with the altered rock fragments are blocks of unaltered tuff and flow rock of the Laguna Springs Volcanic Group shed from exposures at higher elevations north of the altered zone. The relative proportions of altered and unaltered materials depends on proximity to the tuff and flow rock exposures.

Near the source, the proportions are nearly equal, whereas in more distal areas, the unaltered debris constitutes only about 10 percent of the rock fragments. Thus, failure to detect most of the altered areas appears to be due to a combination of factors: poor exposures, moderately dense shrub cover, and dilution of the limonite spectral signature by the addition of unaltered debris.

Veins and pebble dikes were detected in a few particularly well exposed areas, such as the northeast-trending zone located about 3 km south of Sunrise Peak (E, fig. 26), but the widths of most are so small that they are obscured at the MSS spatial resolution by vegetation and unaltered rock debris. In addition, some are not as limonitic as the altered volcanic rocks.

The second main discrepancy between the field-compiled alteration map and the MSS-derived limonitic bedrock map has two sources: (1) argillized rocks are not represented in the field map, and (2) some limonitic, but unaltered rocks are included in the limonitic bedrock map. The most extensive area of argillized rocks is the previously mentioned northeast-trending crudely elliptical pattern extending from the head of Ruby Canyon and Silver Pass Canyon south of the Eureka Standard mine (fig. 2; F, fig. 26). The dominant rock types in this zone are latite tuff and ignimbrite of the Tintic Mountain Volcanic Group but Packard Quartz Latite and isolated areas of monzonite porphyry of the Silver City stock are affected at the northeast and southwest termini, respectively. In all these rocks, the plagioclase phenocrysts are commonly altered to clay minerals, and biotite is

generally replaced by a white mica; in a few less intensely altered areas, biotite is oxidized, but incompletely altered. In general, K-feldspar phenocrysts are unaltered. Light to medium brown limonite stain is widespread, but only locally is the surface coating conspicuous because of its color or thickness. Pseudomorphs after disseminated pyrite, typically about 1 mm across, are present in many exposures. Limonite is slightly less abundant in the northeastern extension into Packard Quartz Latite, and, consequently, the ferric absorption bands are less intense (fig. 11), and the green colored pixels are less conspicuous than elsewhere in the elliptical area (fig. 23).

Argillized latitic tuffs of the Tintic Mountains Volcanic Group underlie an area of several hundred square kilometers in Government Canyon, where they are intruded by numerous dikes, sills, and plugs of Sunrise Peak Monzonite Porphyry (G, fig. 26). Because of bleaching and the presence of moderately heavy limonite stains here, this area is conspicuous in the CRC image (fig. 22), in spite of moderately dense tree and shrub cover. The density of vegetation, especially the shrubs, declines in the more intensely bleached altered areas, however.

Perhaps the most conspicuous argillized area in the CRC image is Big Hill (H, fig. 26). As noted earlier, these argillized rocks are characterized by intense ferric-absorption bands due to widespread

limonite and, locally, alunite and jarosite. Here, argillization pervaded parts of the biotite monzonite bodies, as well as most of the Packard Quartz Latite. Similarly, pervasive argillization also occurs north of Big Hill in the western part of the East Tintic mining district; this district will be discussed in detail in a subsequent section.

The largest argillized body, the latite plug southeast of Copperopolis Creek, is represented in the limonitic bedrock map by a reasonably high density of green pixels where the vegetation is sparse (I, fig. 26). Large parts of this and smaller associated bodies are obscured, however, due to moderately dense pinyon and juniper trees and shrubs. Additionally, these rocks are less limonitic than the altered volcanic and intrusive rocks.

As the in situ spectra show (fig. 7), weak alteration of Packard Quartz latite during the intravolcanic episode of accelerated weathering results in moderately intense ferric absorption bands, mainly due to concentrations of limonite along fractures. Although the limonite commonly occurs as reasonably thick coatings, it is not as conspicuous in the field as the iron-oxide minerals associated with undoubtedly hydrothermally altered volcanic and intrusive rocks because the weakly altered rocks are not bleached. Nonetheless, two extensive zones of these weakly altered rocks are indicated by the CRC image. The largest area is located in a highly fractured zone approximately 1 km north-northeast of Eureka (J, fig. 26). Locally, alteration is more intense than is

typical of this episode, with the plagioclase and biotite being altered.

The other area, situated north of U.S. Highway 50 (K, fig. 26), is more consistent with Lovering's descriptions of these rocks: the rocks are slightly bleached and friable, but plagioclase and biotite are either slightly altered to montmorillonite and limonite or appear essentially unaltered; K-feldspar and quartz are unaltered. Smaller, similarly affected quartz latitic rocks are scattered throughout the areas north and south of this locality.

Although the Paleozoic sedimentary rocks are altered in many places and contain important ore bodies, the exposed bodies are typically small. Besides the halloysite and endellite replacement bodies in Ajax, Dolomite, and Opohonga Limestone in the Dragon mine (L, fig. 26), and the aforementioned deposits between Fremont and Rattlesnake Canyons, the only sedimentary deposit that is clearly identifiable in the CRC image is the Iron King No. 1 (M, fig. 26).

Although detection of the Iron King No. 1 area is, like the Dragon deposit, partially due to mine workings, naturally occurring iron-oxide material litters the surface in the vicinity of this area. Hydrothermal dolomite, though not as widespread as argillized volcanic and intrusive rocks, is common in the northern part of the study area. Neither have well defined ferric bands, but the light colored dolomite spectrum falls off more rapidly towards the blue, and therefore should be more readily detectable (fig. 15). However, the largest area of light

colored dolomite in the East Tintic mining district is located on the southern slope of Mineral Hill (N, fig. 26), and is devoid of green pixels. That these rocks are represented by white pixels in the CRC image is consistent with their generally spectrally flat nature.

The most widespread limonitic unaltered rocks in the study area are Tintic Quartzite and certain Packard Quartz Latite flows. The generally north-trending belt of Tintic Quartzite in the northwestern part of the study area is apparent in the CRC image (O, fig. 26), except in the extreme northwest corner, where the tree cover is especially dense. Locally, the limonite is undoubtedly derived from oxidized pyrite in small veins, but its prevalence and generally uniform distribution suggest that the main source is the hematitic material that characterizes the lower one-third of the unit; an additional source is the iron-bearing accessory minerals in the remainder of the section, that, upon weathering, result in a surface coating of the limonite. Although reflectance spectra are not yet available for these rocks, well defined ferric absorption bands are indicated by the CRC image.

Most of the Packard Quartz Latite weathers to a dull gray or rust brown, and is discriminable in the CRC image from the more limonitic silicified and argillized volcanic and intrusive rocks, as well as rocks affected by intravolcanic accelerated weathering; however, a

generally east-southeast-trending zone of quartz latite flow rock north of U.S. Highway 50 is exceptional in that respect (P, fig. 26). These dense, medium-grained, banded rocks have a pink to purple groundmass, presumably due to the presence of microscopic hematite inclusions, that weather to a light pink and pinkish-tan limonitic surface. Unlike the quartz latitic rocks subjected to intravolcanic alteration, the limonitic stain is very uniform.

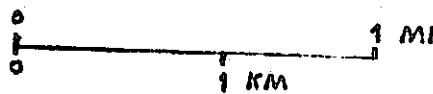
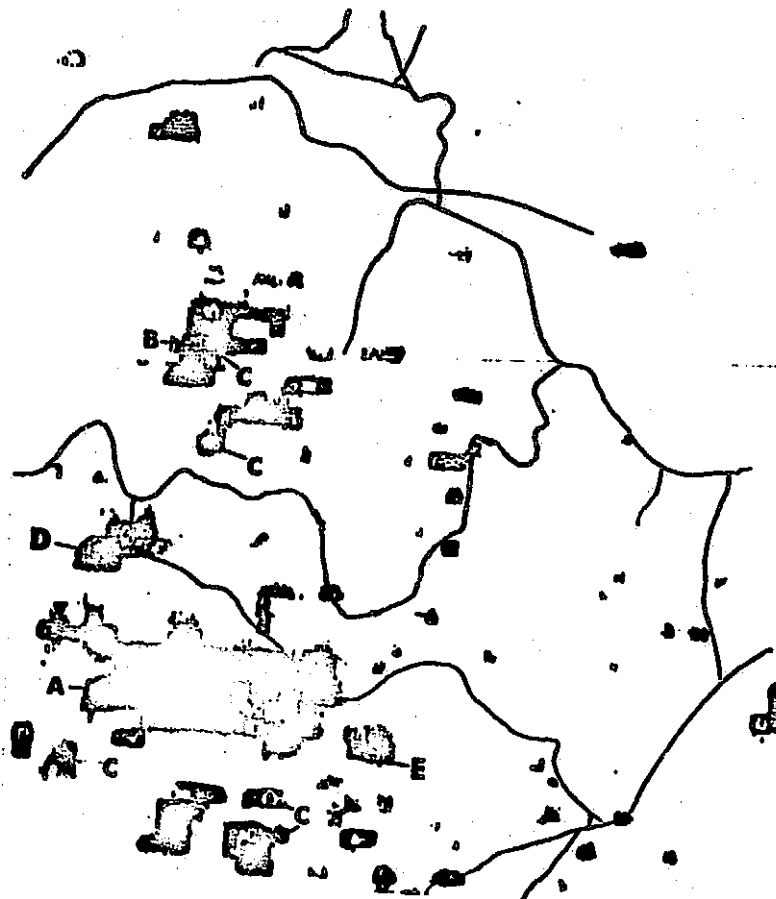
East Tintic mining district - As previously discussed, Lovering (1949) recognized the following types of altered rocks in the East Tintic mining district, that have areal extents larger than one or two MSS pixels:

1. Hydrothermal dolomite
2. Chloritized volcanic rocks
3. Argillized volcanic, intrusive, and sedimentary rocks
4. Silicified sedimentary rocks
5. Calcitic volcanic rocks
6. Pyritized, silicified sedimentary and volcanic rocks
7. Replacement ore bodies

The distribution of these clearly altered rocks are shown in figure 5, but the products of accelerated weathering are not included.

Superposition of the limonitic bedrock map of the East Tintic mining district alteration map permits evaluation of the MSS data for detecting these types of alteration. Because of slight geometric differences, pixel by pixel comparison is not feasible. However, several important conclusions can be reached by examining the general distributions of pixels representing limonitic rocks and the altered rocks. Concentrations of pixels are clearly coincident with the pervasively argillized rocks in the Big Hill and North Hill areas (A and B, fig. 27). Similar agreement is apparent in areas underlain by biotite monzonite porphyry of the Silver City stock (C, fig. 27), although these bodies are much less extensive than the argillized rocks. Surprisingly, the pyritized rocks are only portrayed locally (D, fig. 27), apparently due to dense vegetation in this part of the area.

In contrast with the reasonably good agreement in these areas, several types of alteration in the East Tintic mining district are not represented in the limonitic bedrock map. Areas underlain by calcitic volcanic rocks and hydrothermal dolomite are notably lacking. These results are in keeping with the low ferric iron contents of the calcitic volcanic rocks and hydrothermal dolomite, and hence the absence of intense ferric absorption bands in their representative field spectra (fig. 8a, b, and 15a, respectively). Chloritized volcanic rocks are limited to a few narrow bands, and are therefore difficult to compare with the limonitic bedrock map, but they appear to lack



ORIGINAL PAGE IS  
OF POOR QUALITY

Figure 27. Limonitic bedrock map of the East Tintic mining district.

Enlarged from figure 25 to approximately 1:36,000 scale.

sufficient iron-oxide surface stain to be included in the limonitic bedrock map (fig. 27). Silicified rocks in the district are too small and poorly exposed to be evaluated, and the replacement ore deposits are all concealed by barren rocks.

In a low altitude color photograph (fig. 28), some of the argillized areas, such as Big Hill, appear bleached, but very little color variation is apparent, and, as with the other color photographs (fig. 17 and 18), altered areas that do not have high albedos and unaltered rocks with high albedo are apparent.

See Attached Color Plate



Figure 28. Low-altitude color photograph of the East Tintic mining district.

## Conclusions

These results confirm the positive findings of earlier evaluations of the color-ratio compositing techniques for mapping limonitic altered rocks in south-central Nevada, but they also point out several important limitations of the initial approach. The limitations arise from environmental, geologic, and image processing factors. The most important environmental factor encountered in the East Tintic Mountains study area is substantially denser vegetation cover than is present in south-central Nevada. Measurements of vegetation density indicate that shrub and juniper-pinyon covers denser than 40-50 percent and 33-43 percent, respectively, obscure limonitic altered rocks in the CRC images.

Another important effect of the greater vegetation cover is that, in the optimum CRC image, the MSS 5/6 image was replaced by MSS 4/6. Consideration of schematic frequency distributions for the East Tintic Mountains and south-central Nevada study areas suggests that the lack of enhancement of limonitic rocks in MSS 5/6 ratio images of the present study area is due to the higher frequency of low ratio values representing vegetation. Very severe contrast stretches are needed to shift the limonitic pixels to low film density levels, which result in extremely noisy images. The relative positions of the limonitic rocks and vegetation are similar in MSS 4/6 frequency distribution, but more severe stretches can be applied because of its inherently higher signal to noise content.

The type and density of vegetation appears to be influenced by the presence of certain types of alteration, but the relationship is complicated by many other factors. In general, the density of sage appears to decline in most argillized areas; in silicified areas, there appears to be little change in vegetation cover.

Comparison of the limonitic bedrock map produced from the CRC image with the map showing silicified rocks shows that the silicified rocks are accurately portrayed in the former map, except where they are obscured by vegetation and mixed with unaltered colluvial deposits. Most important is the success that was realized in mapping the pervasively argillized rocks because these are the most widespread altered rocks in the area, but are difficult to map in the field. Evaluation of color photographs obtained from Skylab, high-altitude, and low-altitude aircraft were inadequate for mapping these and the other altered rocks in the area; they were very useful for separating alluvium and bedrock, and for location purposes.

On the other hand, hydrothermal dolomite and chloritic and calcitic volcanic rocks were not portrayed in the limonitic bedrock map, a result that is consistent with their general lack of anomalous amounts of limonite and spectral reflectance characteristics. Some altered rocks, particularly veins and pebble dikes, are too small to be detected by the MSS, except where they are closely spaced and well exposed. Although the topographic relief is moderately high, no altered areas were found to be obscured in the CRC image by topographic shadowing.

An additional geologic limitation is that some unaltered limonitic rocks are included in the limonitic bedrock map; most notable are large areas underlain by Tintic Quartzite and some limonitic quartz latitic rocks. Analysis of in situ spectral reflectance measurements of the latter rocks shows that they should be distinguishable from the altered rocks in the 2.2  $\mu\text{m}$  region because of their lack of hydroxyl-bearing minerals.

Several procedural modifications were instituted to improve the overall mapping accuracy of the CRC approach. Large format ratio images provide much better internal registration of the diazo films and avoids the problems associated with large magnifications required in the initial procedure. Also, use of the Linoscan 204 color-recognition scanner permits accurate consistent extraction of the green pixels representing limonitic rocks. The improvements result in CRC images and limonitic bedrock maps that can be used for mapping at large scales, as well as for small-scale reconnaissance.

### References Cited

- Allen, W. A., and Richardson, A. J., 1968, Interaction of light with a plant canopy: Jour. Opt. Soc. Amer., v. 58, p. 1023-1028.
- Billings, W. D., 1974, Vegetation and plant growth as affected by chemically altered rocks in the western Great Basin: Ecology, 31:62-74.
- Blodgett, H. W., Brown, G. F., and Moik, J. G., 1975, Geological mapping in northwestern Saudi Arabia using Landsat multispectral techniques: NASA Tech. Document No. X-923-75-206, 21 p.
- Goetz, A. F. H., Billingsley, F. C., Gillespie, A. R., Abrams, M. J., Squires, R. L., Shoemaker, E. M., Lucchitta, I., and Elston, D. P., 1975, Application of ERTS images and image processing to regional geologic problems and geologic mapping in northern Arizona: Jet Propulsion Lab. Tech. Rept. 32-1597, 188 p., Pasadena, Calif.
- Hunt, Graham R., 1977, Spectral signatures of particulate minerals in the visible and near-infrared: Geophysics, v. 42, no. 2, p. 275-287.
- Hunt, G. R., and Salisbury, J. W., 1970, Visible and near-infrared spectra of minerals and rocks - I: Silicate minerals: Mod. Geology, v. 1, p. 283-300.
- Hunt, G. R., and Salisbury, J. W., 1971, Visible and near-infrared spectra of minerals and rocks - II: Carbonates: Mod. Geology, v. 2, p. 23-30.

- Hunt, G. R., and Salisbury, J. W., 1974, Remote sensing of rock types in the visible and near-infrared, in Proceedings of the Ninth International Symposium on Remote Sensing of Environment, 15-19 April 1974, Ann Arbor, Mich., p. 1953-1958.
- Hunt, G. R., Salisbury, J. W., and Lenhoff, C. J., 1971, Visible and near-infrared spectra of minerals and rocks - IV, Sulphides and Sulphates: Mod. Geology, v. 3, p. 1-14.
- Hunt, G. R., Salisbury, J. W., and Lenhoff, C. J., 1973, Visible and near infrared spectra of minerals and rocks - VI, Additional Silicates: Mod. Geology, v. 4, p. 85-106.
- Lindgren, Waldmar, and Loughlin, G. F., 1919, Geology and ore deposits of the Tintic mining district, Utah: U. S. Geol. Survey Prof. Paper 107, 282 p.
- Lovering, T. S., 1949, Rock alteration as a guide to ore - East Tintic district, Utah: Economic Geology Mon. 1, 65 p.
- Morris, H. T., 1957, General geology of the East Tintic Mountains and ore deposits of the Tintic mining districts: Utah Geol. Soc. Guidebook 12, p. 1-56.
- Morris, H. T., 1964a, Geology of the Eureka quadrangle, Utah and Juab Counties, Utah: U.S. Geol. Survey Bull. 1142-K, 29 p.
- \_\_\_\_ 1964b, Geology of the Tintic Junction Quadrangle, Toole, Juab, and Utah Counties, Utah: U.S. Geol. Survey Bull. 1142-L, 23 p.
- \_\_\_\_ 1975, Geologic map and sections of the Tintic Mountain Quadrangle and adjacent part of the McIntyre Quadrangle, Juab and Utah Counties, Utah: U. S. Geol. Survey Misc. Inves. Map, I-883.

- Morris, H. T., and Lovering, T. S., 1961, Stratigraphy of the East Tintic Mountains, Utah: U.S. Geol. Survey Prof. Paper 361, 145 p.
- Morris, H. T., and Anderson, J. A., 1962, Eocene topography of the central East Tintic Mountains, Utah, in Geological Survey research, 1962: U.S. Geol. Survey Prof. Paper 450-C, p. C1-C4.
- Morris, H. T., and Mogensen, A. Paul, 1978, Tintic mining district, Utah: Brigham Young Univ. Geol. Studies (in press).
- Raines, Gary L., in press, A porphyry copper exploration model for northern Sonora, Mexico: U.S. Geol. Survey Jour. of Research.
- Rowan, Lawrence C., Wetlaufer, Pamela H., Goetz, Alexander F.H., Billingsley, Fred C., and Stewart, John H., 1974 Discrimination of rock types and detection of hydrothermally altered areas in south-central Nevada by use of computer-enhanced ERTS images: U.S. Geol. Survey Prof. Paper 883, 35 p.
- Rowan, Lawrence C., Goetz, Alexander F. H., Ashley, Roger P., 1977, Discrimination of hydrothermally altered and unaltered rocks in visible and near-infrared multispectral images: Geophysics, v. 42, no. 3, p. 522-535.
- Siegal, Barry S., and Goetz, Alexander F. H., 1977, Effect of vegetation on rock and soil type discrimination: Photogrammetric Engr. and Remote Sensing, v. 43, no. 2, p. 191-196.
- Tower, G. W., and Smith, G. W., 1899, Geology and mining industry of the Tintic District, Utah: U. S. Geol. Survey 19th Ann. Rept (1897-98), pt. 3, p. 601-767.

FOLDOUT FRAME 1

20-000000-000000

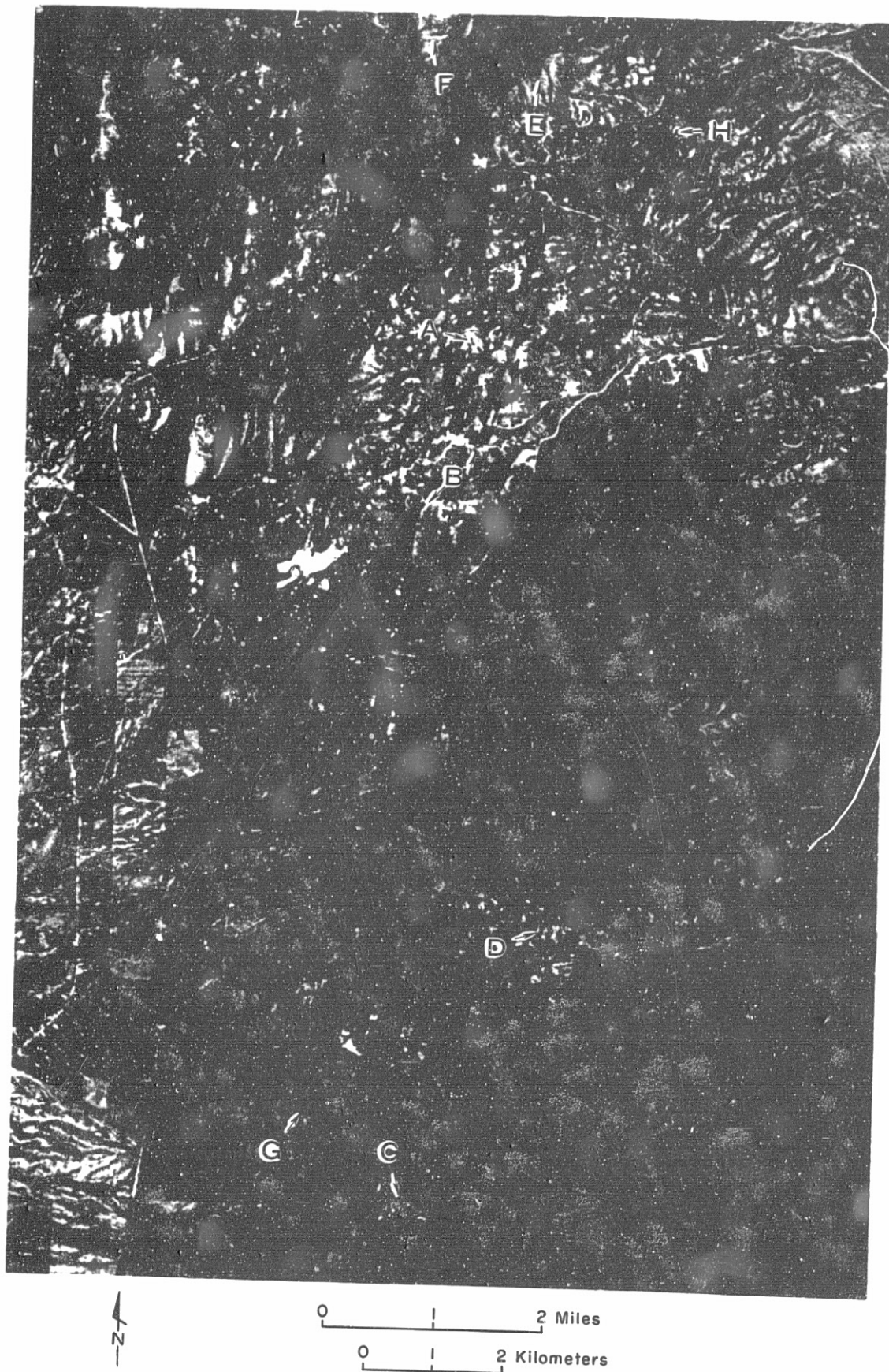
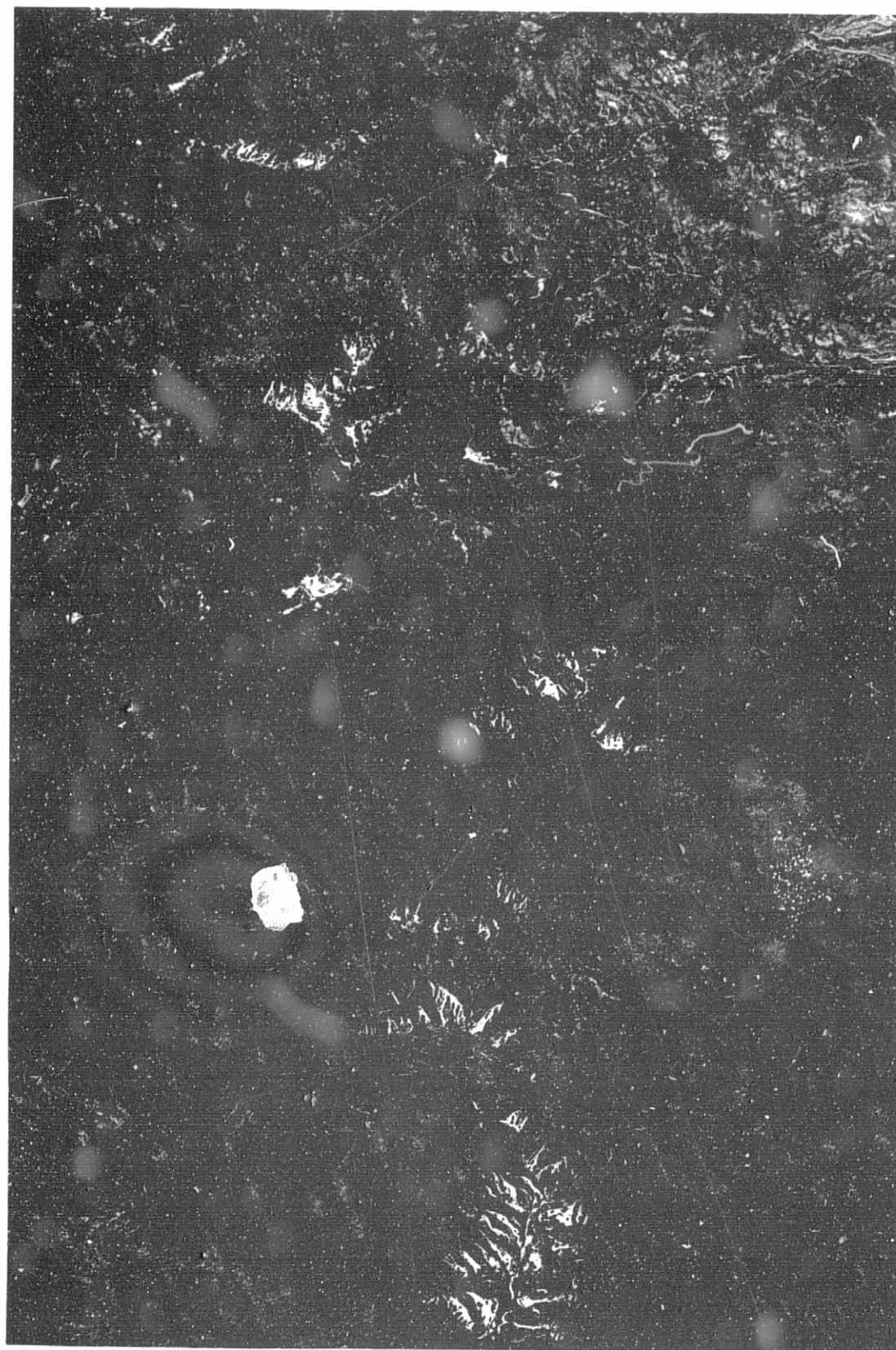


FIGURE 17.—Skylab S190B color photograph of the study area showing high albedo argillized areas A, Big Hill, B, elliptical area, C, latite plug, D, Government Canyon; high albedo sedimentary rocks E, south of Pinyon Peak, F, west of Pinyon Peak; and low to moderate albedo altered areas G, pyritized breccia pipe, and H, silicified area southeast of Pinyon Peak.

0100011000101

ORIGINAL PAGE IS  
OF POOR QUALITY



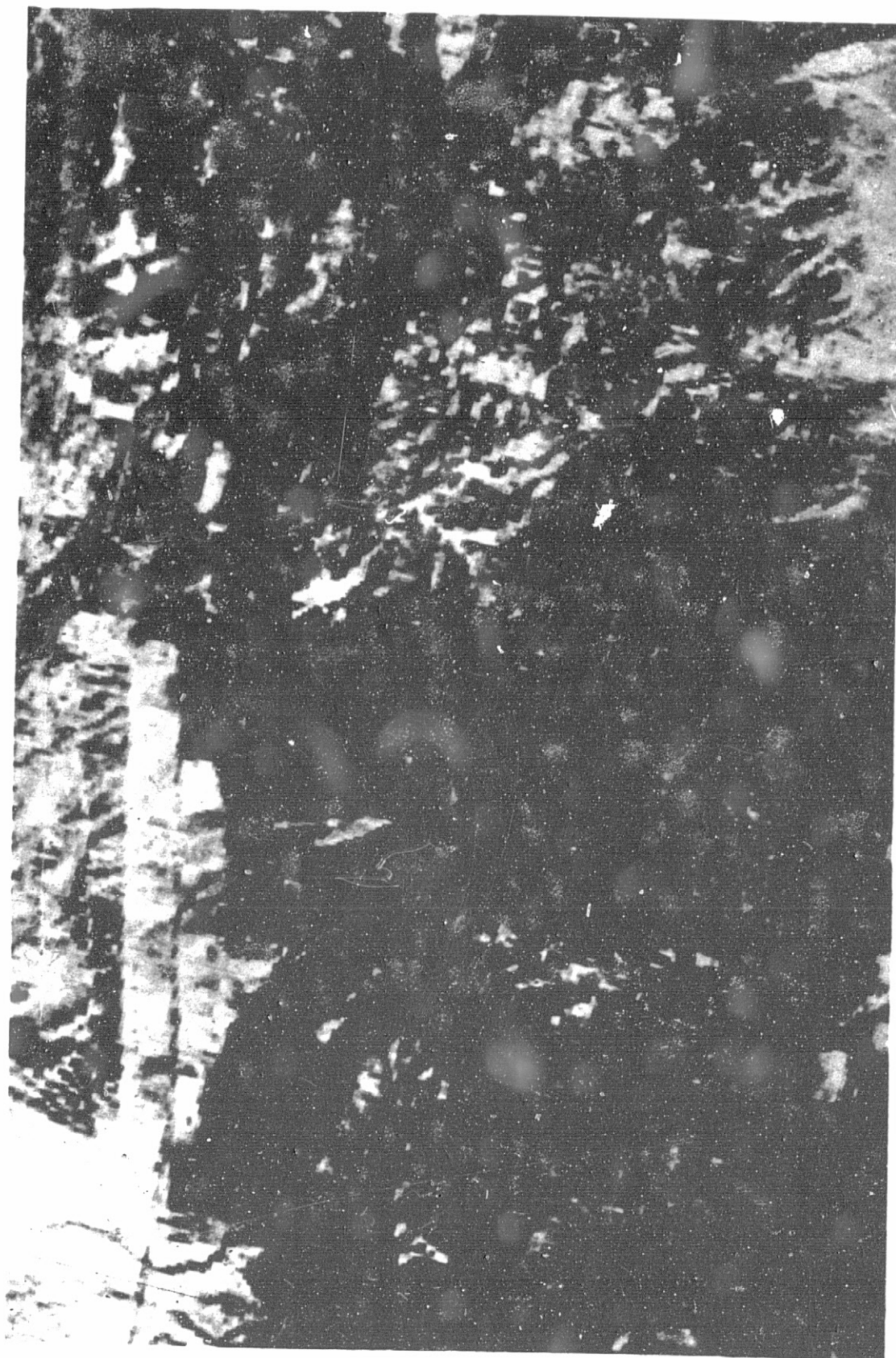
2

0 1 2 Miles

0 1 2 Kilometers

FOLDOUT PAGE 2

FIGURE 18.—High-altitude color photograph of the study area.



FOLDOUT FRAME 3

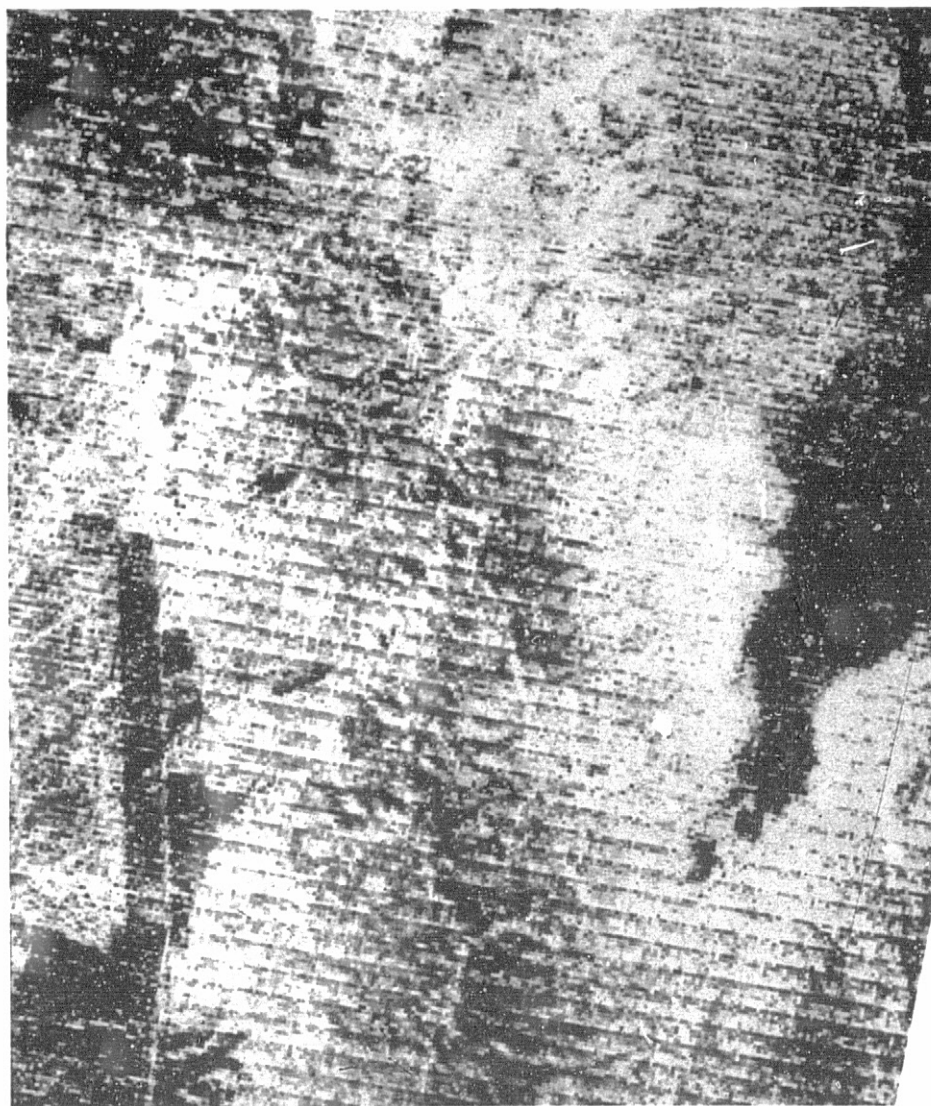
ORIGINAL PAGE IS  
OF POOR QUALITY

N  
↑

0 1 2 Miles

0 1 2 Kilometers

FIGURE 21.—Color-infrared composite image of the study area made in a color-additive viewer using MSS bands 4, 5, and 7 in blue, green, and red, respectively.



0 1 2 Miles

0 1 2 Kilometers

FIGURE 23.—Color-ratio composite image of the study area made using blue, yellow, and magenta diazo colors for MSS ratio images 4/5, 4/6, and 6/7, respectively. ID E-1735-17335. Recorded 28 July 74.

FOLDOUT FRAME

41

FOLDOUT  
FOLDOUT FRAME

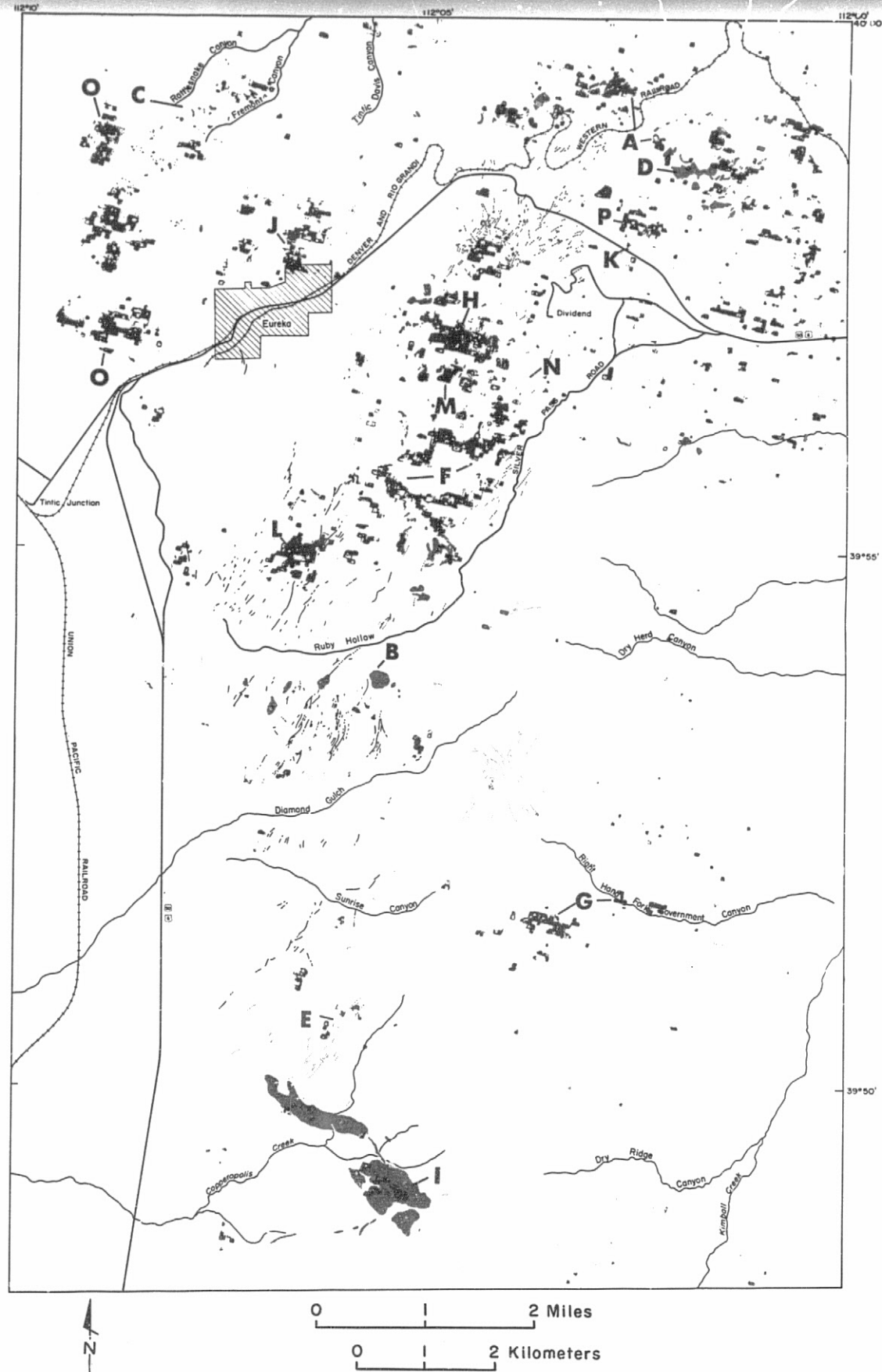
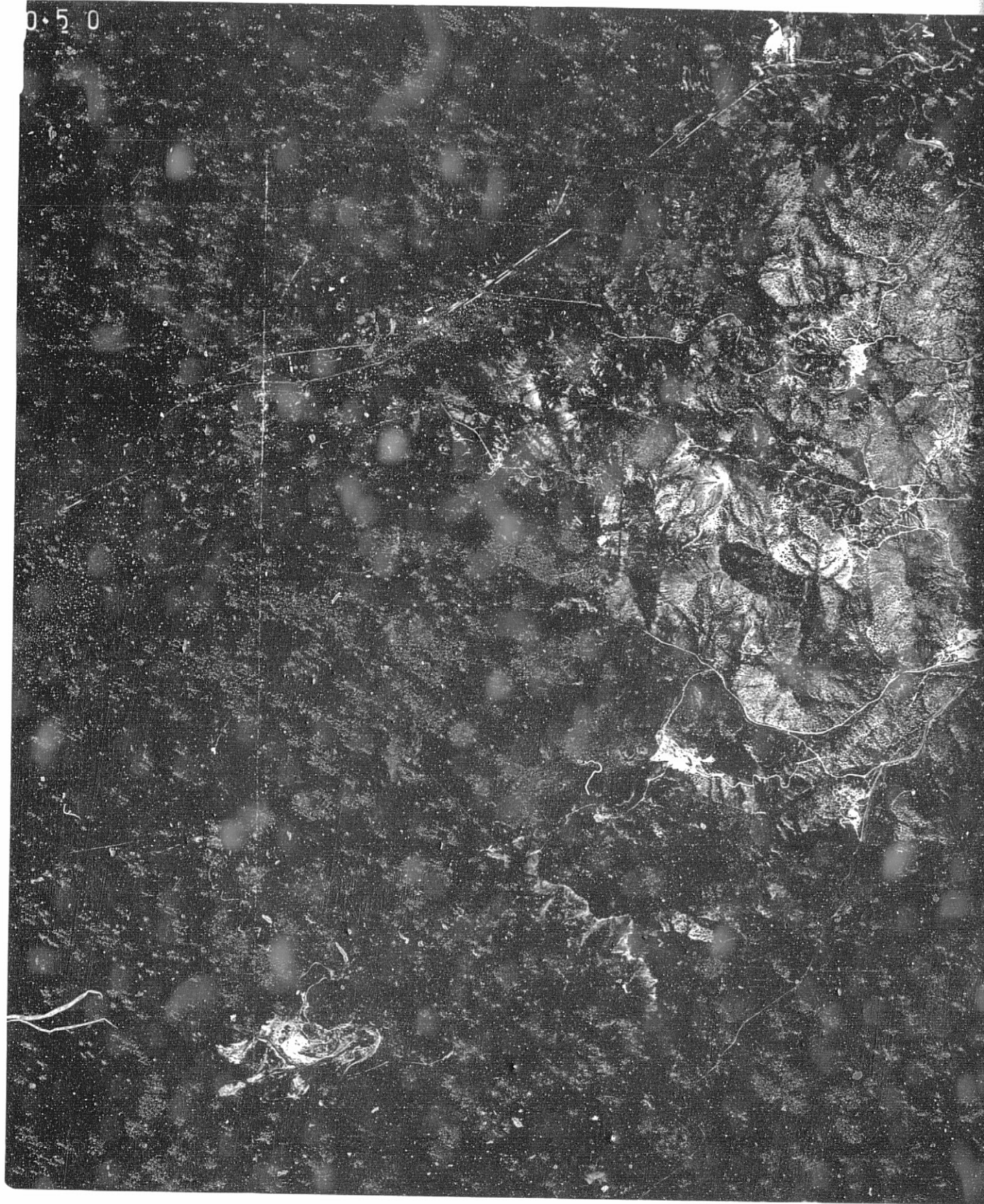


FIGURE 26.—Map of the study area comparing the distributions of altered areas and veins mapped in the field (shown in fig. 4) with pixels representing limonitic rocks (shown in fig. 25). Gray represents altered areas mapped in the field; magenta represents limonitic rocks. A, silicified rocks southeast of Pinyon Peak; B, silicified rocks obscured by vegetation; C, small areas of silicified rocks; D, area of mixed unaltered volcanic and altered volcanic rocks; E, well-exposed vein deposits; F, argillized rocks in crudely elliptical area; G, argillized latitic tuffs; H, argillized quartz latite; I, argillized latite plug; J, limonitic weakly altered quartz latite; K, limonitic quartz latite; L, Dragon mine; M, Iron King #1 mine; N, hydrothermal dolomite; O, north-trending Tintic Quartzite; P, pink quartz latite flow rock.



RESCUT FRAME

N

0 1 2 Miles  
0 1 2 Kilometers

ORIGINAL PAGE  
OF POOR QUALITY

FIGURE 28.—Low-altitude color photograph of the central part of the East Tintic Mountains, Utah. Dashed line shows location of the East Tintic mining district.



06-0500

0 1 2 Miles  
0 1 2 Kilometers

ORIGINAL PAGE IS  
OF POOR QUALITY

FOLDOUT FRAME 7

Low-altitude color photograph of the central part of the East Tintic  
Utah. Dashed line shows location of the East Tintic mining district.